

Inhibitory control of speech production in the human premotor frontal cortex

Received: 8 August 2024

Accepted: 16 January 2025

Published online: 03 March 2025

 Check for updates

Lingyun Zhao  ^{1,2}, Alexander B. Silva  ^{1,2,3,4}, G. Lynn Kurteff¹ & Edward F. Chang  ^{1,2} 

Voluntary, flexible stopping of speech output is an essential aspect of speech motor control, especially during natural conversations. The cognitive and neural mechanisms of speech inhibition are not well understood. Here we have recorded direct high-density cortical activity while participants engaged in continuous speech production and were visually cued to stop speaking. Neural recordings revealed distinct activity in the premotor frontal cortex correlated with stopping speech. This activity was found in largely separate cortical sites from regions encoding vocal tract articulatory movements. Moreover, this activity primarily occurred with abrupt stopping in the middle of an utterance, rather than naturally completing a phrase. Electrocortical stimulation at many premotor sites with inhibitory stop activity caused involuntary speech arrest, which contradicts previous clinical interpretations of this effect as evidence for critical centres of speech production. Together, these results suggest a previously unknown premotor cortical network that supports the inhibitory control of speech, providing implications for understanding both natural and altered speech production.

Speech production research has primarily focused on studying how speech is planned, articulated and maintained^{1–3}, with little focus on how it is voluntarily stopped. However, an important aspect of speech motor control is to immediately stop speaking⁴. Speech utterances consist of organized structures with complicated articulatory movements, yet they can still be terminated at almost any time^{4,5}. Natural conversations often require us to stop speaking before an utterance is finished, for example, after interruption by an interlocutor^{6–8}. Certain speech and communication disorders involve improper or inadequate stopping, such as stuttering^{9–13} and excessive self-directed speech in attention deficit hyperactivity disorder (ADHD)¹⁴. The neural basis that enables immediate speech stopping remains unclear. In line with the focus on planning and maintenance of speech motor commands, it has been believed that disengagement of speech motor signals, critical for planning and coordinating speech production, underlies immediate stopping. Under this framework, neural activity in the premotor and motor cortices is expected to diminish during stopping¹⁵.

Inhibitory control has been found to mediate many brain functions and behaviours in both humans and animals^{16–18}. For example, before executing an action, the motor system is engaged in the preparation and initiation of the movement. If a stop signal occurs early in time, it will quickly suppress the motor output by activating the inhibitory control systems in the brain¹⁹. Here we hypothesize that stopping ongoing, continuous speech production is based on inhibitory mechanisms through specialized neural signals. Previous studies on inhibitory control have identified specific neural pathways that are separate from those that control movement initiation and execution. Most studies have focused on behaviours that require stopping a simple motor movement before it is executed, in the context of response inhibition¹⁹. These studies have identified a cortico-basal ganglia inhibitory circuit, involving structures such as the right inferior frontal cortex (rIFC), pre-supplementary motor area (pre-SMA) and several subcortical regions^{20–26}. In this circuit, neural signals originating from the prefrontal cortex are routed to the basal ganglia through a so-called ‘hyperdirect pathway’^{24–26} and

¹Department of Neurological Surgery, University of California, San Francisco, CA, USA. ²Weill Institute for Neurosciences, University of California, San Francisco, CA, USA. ³Medical Scientist Training Program, University of California, San Francisco, CA, USA. ⁴University of California, Berkeley - University of California, San Francisco Graduate Program in Bioengineering, Berkeley, CA, USA.  e-mail: Edward.Chang@ucsf.edu

then inhibit the motor cortex through thalamocortical projections. The result is a non-selective, global inhibition of ballistic hand movement and speech^{27–29}. Continuous speech production is, however, distinct from simple movements, requiring precise coordination and sequencing of multiple articulators to generate an array of speech sounds^{12,30}. For example, current and upcoming articulatory gestures may influence how quickly the speech output can be stopped⁵. In this study we tested how the brain, more specifically the premotor cortex, implements immediate stopping of continuous speech production (referred to as ‘early stopping’). Studies on motor control have largely focused on the preparation and programming functions in the premotor cortex, and evidence from animal and human studies has implicated inhibitory functions in the same region^{31–34}. Studies on response inhibition and action stopping have also proposed neural mechanisms relying on frontal regions beyond the rIFC and pre-SMA circuits^{35–40}, with recent evidence of inhibitory control in the premotor cortex^{41–47}.

We used high-density electrocorticography (ECoG) to record cortical activity across frontal, parietal, temporal and medial brain regions. This methodology provided extensive spatial sampling and fine temporal resolution to track millisecond-level dynamics that are essential for both speech production and stopping. Participants performed a task where they were required to immediately start and stop speaking in response to visual cues. We found neural populations across the premotor cortex with robust activations during early stopping. We next demonstrated that this activity was largely specific to early stopping and rarely occurred during the natural passive stop at the end of a phrase. Inhibitory premotor populations did not overlap with populations important for controlling articulators during production. Finally, we found an overlap between sites showing task-related stop activity and those causing speech arrest when stimulated. Together, these results provide important evidence for a distinct, causal premotor circuit for inhibitory speech motor control that has not been described previously, underscoring the necessity of adding inhibitory processing to current models of speech production.

Results

To study the neural mechanism for stopping ongoing speech production, we asked participants to perform a speech production task with early stopping guided by a visual cue (‘speech stopping task’). In total, 13 participants (ten left hemisphere (LH) and three right hemisphere (RH)) were included in the analysis. All participants had grid coverage over the lateral premotor cortex, with some having additional frontal, parietal or temporal coverage. A subset had coverage on the medial cortical surface (five LH, three RH). On each trial, a visual cue indicated when participants should start and stop their speaking, where the speech production task was to recite the days of the week at a normal pace (Fig. 1a). Participants were instructed to stop speaking immediately when the stop cue was presented. The time difference between the stop cue and the acoustic stop of speech is referred to as the ‘stop reaction time’ (SRT). Participants finished between 62 and 104 trials in total across two or three blocks. Across all participants, early stopping was successfully achieved (Fig. 1b, top, and Extended Data Fig. 1a). Before stopping, participants spoke in a continuous manner, evidenced by short gaps between utterances (Fig. 1b, bottom, and Extended Data Fig. 1b,c). We excluded trials with SRTs shorter than 0.1 s where participants may have stopped at or before the stop cue by coincidence. We also excluded trials with long SRTs that were outliers in the distribution (Extended Data Fig. 1a; details are provided in the Methods).

Activation of the premotor cortex for early stopping

The premotor cortex on the lateral brain surface includes the anterior part of the precentral gyrus and the posterior part of the inferior frontal gyrus (IFG) and the middle frontal gyrus (MFG). We first asked if the premotor cortex showed activity (high-gamma amplitude (HGA); 70–150 Hz) that was time-aligned to key moments when participants

were cued and executed speech production and stopping. We aligned the neural data to the go cue, speech start and the stop cue, respectively (Fig. 1c). In an example electrode in the premotor part of the precentral gyrus, we found that HGA increased during the stopping phase of the trial (paired two-sided *t*-test, false discovery rate (FDR) corrected, $q = 0.05$) (Fig. 1c, top row; details are provided in the Methods). A second example electrode in the posterior IFG showed sustained activation during production (production activity) and a further increase in activity after the stop cue (Fig. 1c, middle row). A third example electrode in the precentral gyrus showed increased activity during production, but no further activation after the stop cue (Fig. 1c, bottom row). We refer to the increased activity after the stop cue as stop activity, regardless of whether production activity was also present. We also found that some electrodes showed increased activity after the go cue (that is, go activity; Extended Data Fig. 2). For electrodes showing stop activity, 27% (91 out of 337 electrodes) also showed go activity (Extended Data Fig. 2b,d). To identify the specific neural signals associated with stopping, beyond those activated by a common process following either stop or go cues (such as signals reflecting a state change in the task), we define stop electrodes as those showing significant stop activity that is also significantly stronger than their go activity. We restrict our subsequent analysis to these stop electrodes. The existence of stop electrodes suggests an inhibitory function of these cortical sites. The inhibitory function may be exclusive to a cortical site, or it can co-localize with other functions, such as production.

We observed a similar pattern of stop activity from each participant, with the location of stop electrodes primarily found in the premotor and prefrontal regions, including the ventral to middle precentral gyrus, parts of the IFG, MFG and medial frontal regions (for example, pre-SMA; Fig. 1d and Extended Data Fig. 3). The overall anatomical areas where stop electrodes were found appeared to be similar to those where production activity was found (Fig. 1d), with the most overlap in the precentral gyrus (Fig. 1e), but some difference was observed in individual brains (Extended Data Fig. 3). To quantify the overlap between stop activity and production activity at the level of individual electrodes, we compared the magnitude of these activities within individual electrodes (Fig. 1f). Most electrodes showed either stop activity only (Stop+/Prod−, $N = 233$) or production activity only (Stop−/Prod+, $N = 325$). A small fraction showed both (Stop+/Prod+, $N = 48$, 17% of all stop electrodes). Accordingly, there is little overlap between stop activity and production activity at a fine spatial scale. These results indicate there are distinct neural populations in the premotor cortex that control inhibition and motor movements during ongoing speech.

Stop activity is specific to early stopping

We asked whether stop activity reflects a volitional control of speech stops (that is, early stopping) or whether this activity is also found when participants naturally complete their intended speech (that is, natural finish). A subset of participants ($N = 5$) completed the speech stopping task and a task in which they spoke aloud natural English sentences³⁰. In the sentence reading task (Methods), one sentence was presented on the screen in each trial and participants started reading it aloud following a go cue. They stopped their speaking whenever they finished the sentence and there was no stop cue. We first examined electrodes that were classified as Stop+/Prod− in the speech stopping task and found electrodes where there was an increase in activity during early stopping, but no change in activity during natural finish, when aligned to the time of speech stop (Fig. 2a). For all the Stop+/Prod− electrodes, the majority (83%, 71/86) were activated only in early stopping ($P < 0.001$, two-sided sign test; Fig. 2b and Extended Data Fig. 4a). We compared the two conditions in Stop+/Prod+ electrodes and observed electrodes that also showed an increase in early stopping, but not in the natural finish (Fig. 2c). Similar to the Stop+/Prod− electrodes (Fig. 2a,b), the Stop+/Prod+ electrodes were more likely to show stop activity only

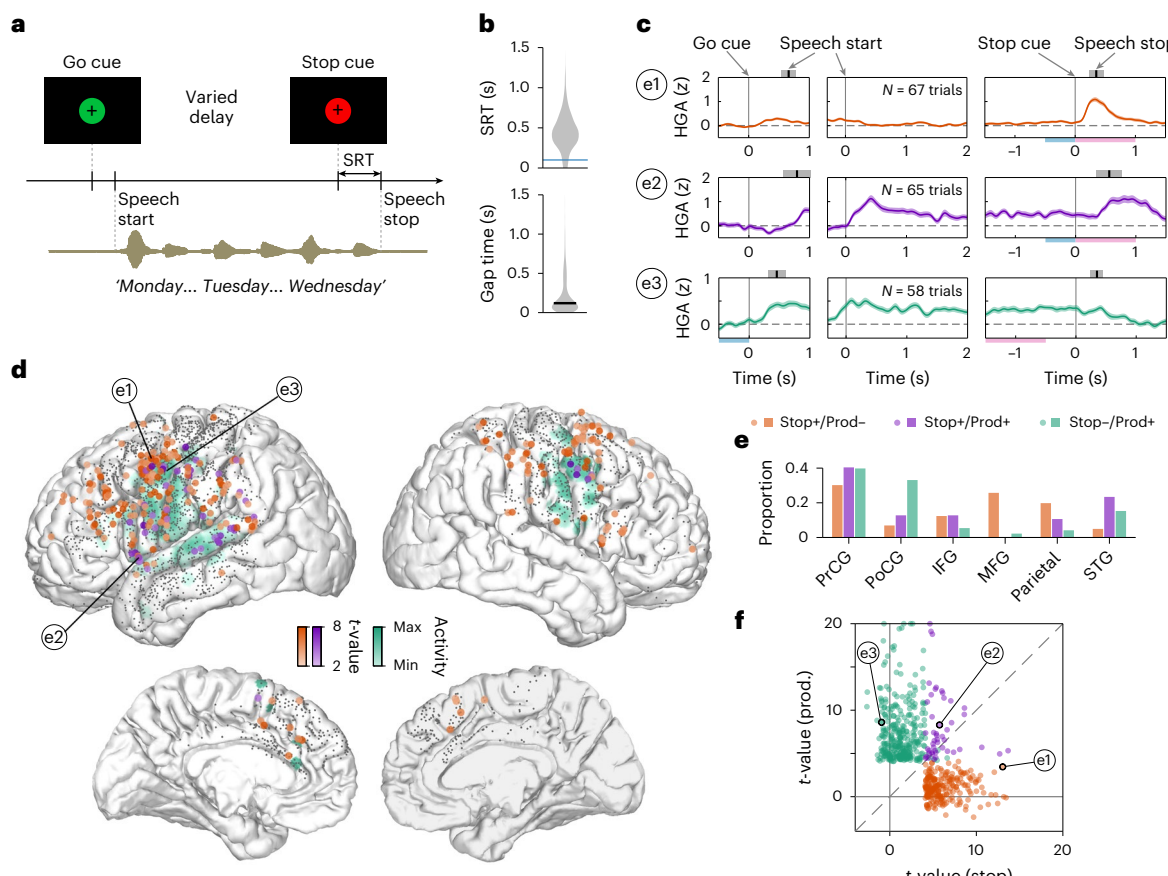


Fig. 1 | Premotor neural activation during speech stopping. **a**, Schematic of the speech stopping task. The go and stop cues are represented by green and red circles, respectively. SRT, stop reaction time. **b**, Top, distribution of SRTs from all trials tested across participants ($N = 1,160$ trials). Blue line denotes lower threshold (0.1 s) for trials included in subsequent neural analyses. Bottom, distribution of gap time between continuous utterances ($N = 2,095$ gaps). Thick black line denotes the median. **c**, Example electrodes demonstrating three types of neural activity pattern (mean \pm s.e.m.). HGA (z), high-gamma amplitude (z-score). Top row, electrode (e1) showing increased activity after the stop cue but no activity during production. Middle row, electrode (e2) showing increased activity during production and an additional increase after the stop cue. Bottom row, electrode (e3) showing increased activity during production but no additional activation after the stop cue. Activity is aligned to three different time points: go cue, speech start and stop cue. The time of speech start and speech stop is marked above the panels (mean \pm s.d.). Blue bars below the panels illustrate the baseline periods. Pink bars illustrate the time periods for

testing functional activity. The blue and pink bars for the top and middle rows are for testing stop activity. Those for the bottom row are for testing activity during production. **d**, Location of all stop electrodes (coloured circles) across participants (ten LH, three RH) plotted on an average brain (MNI-152). Colour intensity indicates the magnitude of activity (t -value). Orange indicates stop electrodes with no production activity (Stop+/Prod-). Purple indicates stop electrodes with production activity (Stop+/Prod+). Green indicates activation map generated from electrodes that showed activation during production, with stop electrodes excluded (Stop-/Prod+). Grey dots indicate the electrode coverage. **e**, Proportion of electrodes found in different brain regions, relative to the total number of electrodes for each of the three types. PrCG, precentral gyrus; PoCG, postcentral gyrus; IFG, inferior frontal gyrus; MFG, middle frontal gyrus; Parietal, parietal cortex; STG, superior temporal gyrus. **f**, Scatter plot of activity magnitude during stopping and production, including the three types of electrode. Each circle indicates a single electrode. A few electrodes with magnitude larger than the axis limit are plotted on the border.

in the early stopping case (74%, 17/23; $P = 0.035$, two-sided sign test; Fig. 2d and Extended Data Fig. 4a).

To test the natural finish condition with a similar framework as the speech stopping task, one participant (S13) performed a control task where only 'Monday' to 'Thursday' were spoken in each trial (Extended Data Fig. 4b). In most trials, the stop cue occurred after the end of 'Thursday' (natural finish). In other trials, the stop cue occurred before the end of 'Thursday' and the participant had to stop immediately (early stopping). There was no significant increase in activity after the stop cue in the natural finish condition (Extended Data Fig. 4c). A few electrodes showed activation around the time of speech stop during the natural finish, but the majority of electrodes were only activated during early stopping (82%, 18/22; $P = 0.004$, two-sided sign test; Extended Data Fig. 4d). Together, these results suggest that high-gamma stop activity is predominantly specific to the early stopping condition and thus may be part of volitional control to actively inhibit ongoing speech.

Previous studies have found beta-band activity as a neural signature for response inhibition²⁰. Here we tested whether the beta-band signal also showed specific activity during early stopping of speech. During motor movement, the beta-band signal generally shows suppression in a wide range of sensorimotor and frontal areas. When movement finishes, beta-band activity shows an increase. In our speech stopping task, we observed increased beta-band activity around the time of speech stop (Fig. 2e and Extended Data Fig. 4e). In an example electrode, beta-band activity showed an increase for both early stopping (speech stopping task) and a natural finish (sentence reading task), after the time of speech stop (Fig. 2e). Among all electrodes showing increased beta-band activity for stopping, in only a small proportion was this increase found in early stopping but not natural finish (17%, 99/586, $z = 16.0$, $P < 0.001$, two-sided sign test; Fig. 2f, orange markers). This contrasts sharply with the high-gamma stop activity. This suggests that beta-band activity is not specifically related to early stopping.

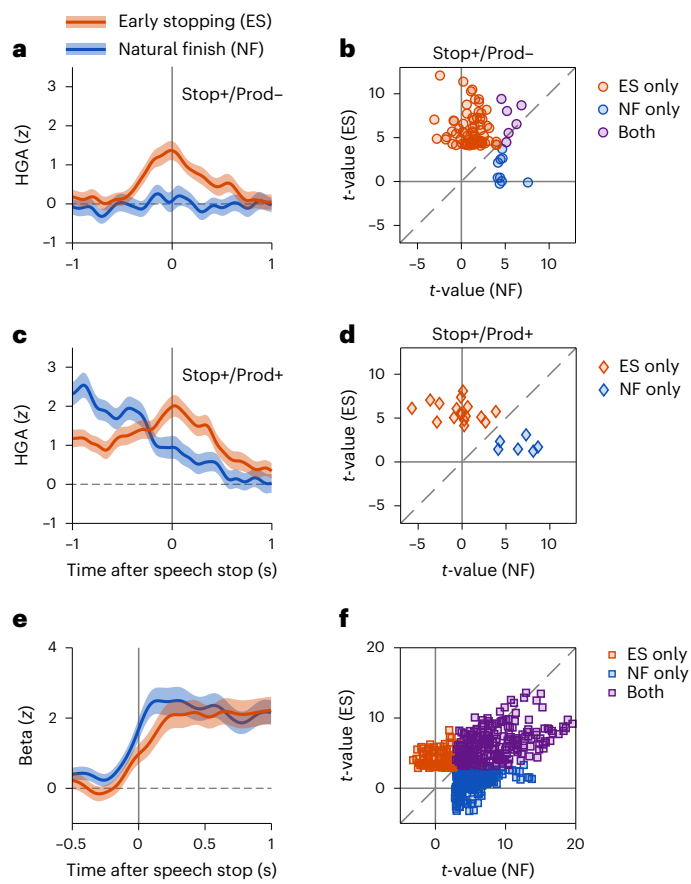


Fig. 2 | Stop activity primarily found in early stopping. **a,c**, Example electrodes that show high-gamma stop activity (mean \pm s.e.m.) during early stopping (ES), but not a natural finish (NF); example electrode with no production activity (**a**) and example electrode with production activity (**c**). **b,d**, Scatter plot of high-gamma activity magnitude during ES and NF for all electrodes showing stop activity in either condition ($N = 5$ participants tested for both ES and NF), where each marker indicates a single electrode: electrodes with no production activity (**b**) and electrodes with production activity (**d**). **e**, Example electrode showing increased beta-band activity (mean \pm s.e.m.) during ES and NF. The location of this electrode is shown in Extended Data Fig. 4e. **f**, Scatter plot of beta-band activity magnitude during ES and NF for all electrodes showing increased activity in either condition. Each marker indicates a single electrode.

Timing of stop activity correlates with stop action

The increased activity after the stop cue may be induced as a response to the cue or related to control of the stop action. To delineate the two possibilities, we performed temporal correlation analysis across single trials and found electrodes showing characteristics of these two types of function (Fig. 3). We only included Stop+/Prod– electrodes to avoid potential confounding of correlation stemming from articulatory signals at the end of speech. We also excluded one participant (S13) in the subsequent analysis because the participant mainly performed the control task, having a limited number of trials for the speech stopping task. Figure 3a shows one example electrode in which the activity was found to be time-locked to speech stop (action-related). To quantify this relationship, we identified the dominant activity time, an alternative measure of peak time, for the single trials that showed relatively strong activities (Methods). The dominant activity time captures when the major event of neural activity occurs but without being biased by random fluctuations in single trials. This electrode showed a significant correlation between the dominant activity time and the stop reaction time (Fig. 3c). In another example electrode, HGA was found to be time-locked to the stop cue (cue-related, Fig. 3b). The dominant activity time showed no correlation with the stop reaction time (Fig. 3d), and

the variation of dominant activity time is small (s.d. < 0.15 s). In total, 74 electrodes showed action-related stop activity and 52 electrodes showed cue-related stop activity. The remaining electrodes with stop activity were not correlated with either action or cue and were referred to as ‘other’ ($N = 93$ electrodes; Extended Data Fig. 5a). The location of ‘other’ electrodes was similarly distributed across several brain regions, with most electrodes in the precentral gyrus and MFG (Extended Data Fig. 5b,c).

We next tested whether stop activity preceded and led to the stop action, which would be supported by electrodes with increases in activity before the time of speech stop but after the stop cue. We first aligned the neural activity to the stop cue and calculated the averaged normalized activity for each electrode based on type (Fig. 3e and Extended Data Fig. 5d). Electrodes with both cue-related and action-related activity showed an increase in activity well before the time of speech stop. The cue-related activity reached its peak earlier than the action-related activity. On a trial-by-trial basis, we aligned the neural activity of individual electrodes to the time of speech stop for the corresponding trial and obtained the activation start time. For the majority of electrodes, the activation start time was earlier than the time of speech stop (94% for cue-related and 73% for action-related activity; Fig. 3f). We also analysed individual electrodes’ activation peak time from the averaged activity aligned to the time of speech stop. The cue-related electrodes showed an earlier peak time than the action-related electrodes ($z = 4.35$, $P < 0.001$, two-sided rank-sum test; Fig. 3g). Stop activity for most electrodes preceded the stop reaction time, suggesting that this activity predicts or drives the stop action, rather than being a passive response. The difference in the peak time of the stop activity suggests that neural signals may track different events relevant to the stopping behaviour in their temporal order. The cue-related activity may be involved in identifying the need to stop speaking, which constitutes an early stage. In contrast, later-stage action-related activity may be involved in forming the stop command and controlling the execution of speech stopping. For the electrodes belonging to the ‘other’ type, a majority do not have a clear temporal activity pattern, suggesting that they may be engaged in various cognitive processes during stopping.

Stopping in the middle of a word modulates stop activity

To further understand the relationship between stop activity and the specific behavioural consequences of speech stopping, we compared instances where participants stopped speaking after the end of a word (end-of-word) and in the middle of a word (midword, Fig. 4a). A subset of participants ($N = 8$; seven LH) generated sufficient midword trials and were included here. We only examined the Stop+/Prod– electrodes to avoid potential confounds from articulation signals associated with stopping midword. When aligning HGA to speech stop, one example electrode showed stronger stop activity in midword trials than in the end-of-word trials ($P < 0.05$, cluster-based permutation rank-sum test; Fig. 4b). Electrodes showing a similar effect were found across multiple participants ($N = 7$, all LH) and we referred to this difference in activity as the stop-type effect. The HGA was always found to be stronger in midword trials than end-of-word trials (except for two electrodes from one participant in the superior temporal gyrus (STG), not shown here as they are not representative). The region with the largest number of electrodes showing the stop-type effect was the precentral gyrus ($N = 12/31$; Fig. 4c). We next asked whether this activity difference occurred before or after the speech stop. About half of the electrodes started to show activity differences before the time of speech stop ($N = 14$; Fig. 4d), with the precentral gyrus containing most of them ($N = 9$). Therefore, the additional activity found in these electrodes may signal a neural control that led to midword stopping rather than a response to the stopping behaviour. At the population level, we used all Stop+/Prod– stop electrodes for each participant to predict whether stopping within single trials was at midword or end-of-word. A linear

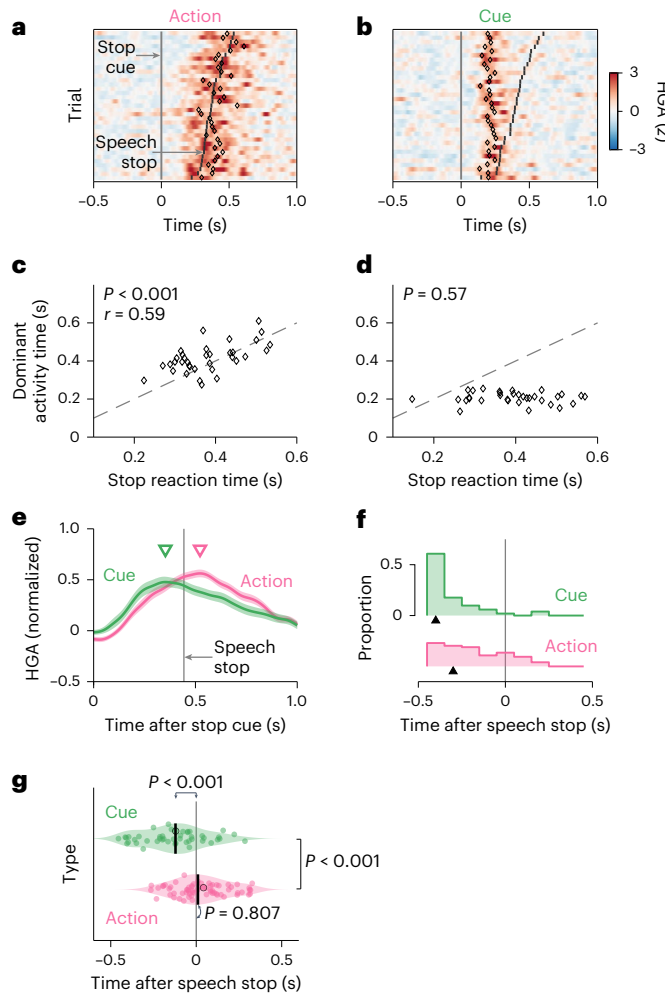


Fig. 3 | The timing of stop activity suggests a neural process leading to speech stop. **a,c**, Example electrode showing high-gamma activity correlated with the action of speech stopping. **a**, Each row indicates a trial, sorted by the stop reaction time. The black diamond marks the dominant activity time (an alternative measure of peak time; Methods). Only trials with strong activity, allowing for identification of a dominant activity time, are shown. The location of the electrode is labelled in Extended Data Fig. 5b. **c**, Scatter plot showing correlations between dominant activity time and stop reaction time. The dashed line is the identity line. **b,d**, Example electrode (as in **a,c**) showing activity correlated to the stop cue rather than the action of speech stopping. **e**, Averaged normalized activity (mean \pm s.e.m.) from electrodes with cue- and action-related activity, time-aligned to the stop cue. Triangles indicate peak time in the smoothed activity pattern. Vertical line denotes the median speech stop time across participants. **f**, Distribution of the activation start time for individual electrodes relative to speech stop. Black triangles indicate the activation start time of the example electrodes in **a–d**. **g**, Distribution of the peak activation time for individual electrodes, relative to speech stop ($N = 46$ electrodes with cue-related activity; $N = 67$ electrodes with action-related activity). Each coloured circle indicates an electrode. Black open circles denote example electrodes in **a–d**. Short black bars indicate medians. Comparisons between the medians and time zero are indicated by double arrows. The median of the peak activation time of the cue-related electrodes is significantly earlier than time zero ($P < 0.001$, two-sided sign test). However, this is not true for the action-related electrodes ($P = 0.807$, two-sided sign test). The peak activation time of the cue-related electrodes is earlier than that of the action-related electrodes ($P < 0.001$, two-sided rank-sum test).

classifier generated predictions significantly above chance for six out of eight participants (Fig. 4e). These results indicate that stop activity distinguishes how a stop was made in each trial, and further confirms that stop activity drives the behaviour of speech stopping.

Separate brain region for encoding speech articulation

Neuronal populations in the sensorimotor cortex were found to encode articulatory kinematic trajectories (AKTs) during continuous speech production³⁰. We sought to determine the relationship between stop activity and the activity that controls articulation. For a subset of participants ($N = 9$) we were able to use acoustic-to-articulatory inversion (AAI) algorithms to infer the kinematics of vocal tract movements (Methods). Figure 5a shows an example electrode that encodes AKTs. We extracted 13 features to quantify the AKTs and used an encoding model to predict HGA from these features (Methods). Figure 5b shows the fitted temporal filter of this example electrode, which illustrates the specific articulatory kinematic pattern to which the electrode is sensitive. The quality of the model fit was evaluated by the correlation between predicted and actual HGA and was high ($r = 0.69$). Most of the electrodes that strongly encoded AKT ($r > 0.2$) were located near the central sulcus and the postcentral gyrus (Fig. 5c and Extended Data Fig. 6). By contrast, stop electrodes were mostly located anterior to the AKT-encoding electrodes ($z = 7.99$, $P < 0.001$, two-sided rank-sum test; Fig. 5c,d and Extended Data Fig. 6). To further characterize the extent of overlap between the two populations, we plotted the magnitude of stop activity against the correlation coefficient in the AKT-encoding models for all stop electrodes (Fig. 5e). Electrodes showing strong stop activity (large t -values) did not show strong encoding of AKT features (large r). This suggests that stop electrodes are localized to cortical regions largely separate from AKT-encoding electrodes and that these two groups of activity overlap little on the individual electrode level. Therefore, our data suggest that stop electrodes are not encoding information about specific articulator movements during speech production.

Stopping in midword trials was found to have stronger stop activity than in end-of-word trials, indicating that some stop activity may specifically interact with speech articulatory control. We next asked whether stop activity influences the AKT-encoding activity for early stopping. We calculated Granger causality as a measure of directed functional connectivity before and after the stop cue based on raw neural signals between pairs of electrodes of the two groups (Methods). We used two consecutive windows directly after the stop cue to quantify the change in Granger causality. Rather than comparing Granger causality between two opposing directions, here we compared Granger causality across time windows within the same direction. For the stop electrodes in the premotor cortex, there was a significant increase in Granger causality towards AKT-encoding electrodes in the [0.5, 1]-s window post stop cue compared to baseline ($P < 0.05$, repeated measures analysis of variance (ANOVA), post hoc analysis with Bonferroni corrections; Fig. 5f, left panel). No significant increase in Granger causality above baseline was found in the other direction for these two groups of electrodes (Extended Data Fig. 7a). As a control analysis, stop electrodes in the temporal-parietal region, including the supramarginal gyrus (SMG) and STG, did not show a significant increase in Granger causality towards AKT-encoding electrodes (Fig. 5f, middle panel). We further compared Granger causality between midword and end-of-word trials. For most electrode groups included in the analysis, Granger causality in both directions was larger for the midword trials than for the end-of-word trials ($P < 0.05$, two-sample t -test; Extended Data Fig. 7b). This suggests that the neural network showed higher connectivity when stopping in the middle of a word than when stopping at the end of a word.

Finally, we asked whether the lateral premotor stop activity was related to or originated from neural populations in medial regions, such as pre-SMA, given prior knowledge that pre-SMA contributes to response inhibition. The Granger causality from electrodes showing stop activity in the medial regions to those in the premotor cortex did not show a significant change after the stop cue (Fig. 5f, right panel). It is thus unlikely that the stop activity in the lateral premotor cortex was simply driven by communication from the medial cortex. Rather,

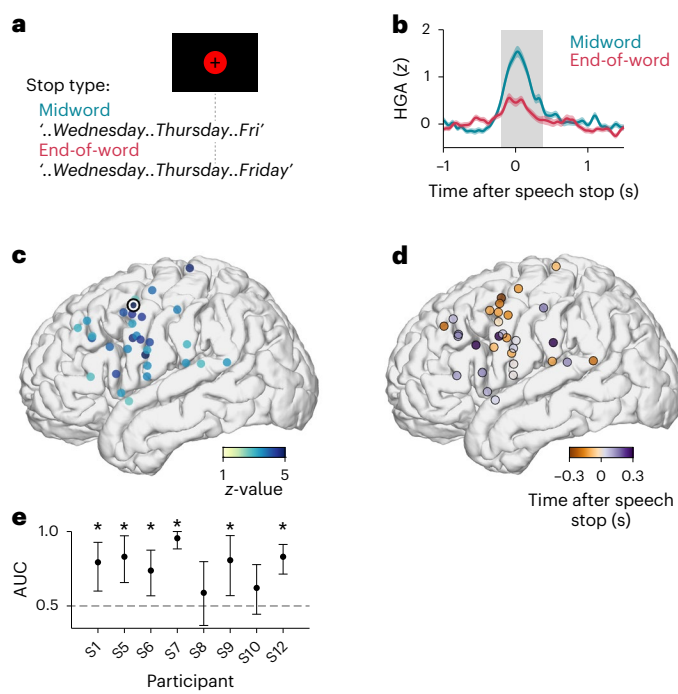


Fig. 4 | Modulation of stop activity by ending words. **a**, Illustration of two types of stopping. In some trials, stopping occurred in the middle of a word (midword). In other trials, stopping occurred after finishing an entire word (end-of-word). **b**, Stop activity of an example electrode (mean \pm s.e.m.). Midword trials showed stronger high-gamma activity than end-of-word trials. The grey shaded region indicates the time period with significant difference between midword and end-of-word trials. **c**, Spatial location and the effect size of electrodes, showing a significant increase in high-gamma activity for midword compared to end-of-word trials, similar to **b**. The black-and-white circle indicates the example electrode in **b**. **d**, Spatial location and the earliest time when electrodes show the stop-type effect, which is illustrated by the left border of the shaded region in **b**. **e**, Classifier performance (mean \pm 95% confidence interval (CI)) for each participant, where stop type was predicted by population activity of all stop electrodes (excluding those with activity during production). AUC, area under the receiver operating characteristic (ROC) curve. Asterisks indicate significant differences from the chance level (dashed line), determined by the CI not overlapping with the chance level.

evidence points to intrinsic neural populations in the lateral premotor cortex that drive early stopping behaviour through communication with AKT-encoding populations.

Partially overlapping location for hand movement stopping

In proposed models for response inhibition, a shared neural circuit is responsible for stopping movements of different modalities²⁹. Here we tested whether early stopping of ongoing speech production and hand movement shared the same mechanism. A subset of participants performed a hand movement stopping task in which they pressed a button repetitively after the go cue and released it immediately after the stop cue ($N = 9$ participants, eight LH, one RH; only LH data are included, 54–71 trials finished by each participant). We followed the same criterion to identify stop electrodes as was used for speech, and used the selectivity index to quantify whether single electrodes had stop activity for speech production, hand movement or both. All stop electrodes were included in this comparison. The electrodes showing stop activity for speech but not hand ('speech only') were found towards the ventral and middle part of the precentral gyrus, IFG and MFG regions (Fig. 6a, left panel, red circles). It is worth noting that electrodes with stop activity for both speech and hand ('both') were also found in the ventral and middle precentral regions (Fig. 6a, left panel, blue circles).

The electrodes with stop activity for hand but not speech ('hand only') were primarily found in the dorsal part of the precentral gyrus (Fig. 6a, left panel, green circles). On the medial side, the distribution of these three types of activity did not show any spatial pattern (Fig. 6a, right panel). The distributions of 'speech only' and 'both' electrodes along the dorsal–ventral axis overlapped, whereas the distribution of 'hand only' electrodes was largely found more dorsally (Fig. 6b). This result suggests that the ventral and middle premotor areas may show an overlap of stop activity across multiple motor modalities, such as speech and hand movement, although many individual sites within these areas still show stop activity specific to speech.

Correlation between stop activity and speech arrest

In clinical practice, neurosurgical patients sometimes undergo functional brain mapping using electrocortical stimulation. Speech arrest, a complete cessation of speech upon stimulation, has been traditionally interpreted as an interruption of neural signalling for speech articulation or planning^{48,49}. The identification of speech arrest sites has long been assumed to be specific to 'Broca's area' by many researchers and clinicians^{50–53}. However, an alternative explanation for speech arrest is that stimulation evokes an inhibitory mechanism that stops speech. Here we investigate these possibilities by comparing the spatial location of stop activity with speech arrest. A subset of LH participants with the speech stopping task underwent electrocortical stimulation through the same ECoG grid for clinical purposes ($N = 8$ participants). Participants counted aloud continuously while stimulation was delivered at a time that was unpredictable to the participants. We characterized two types of stimulation effect: speech arrest and speech error/orofacial effect (Fig. 7a). Speech arrest was identified when speech phonation was completely absent and there was no major orofacial movement. Speech error was identified when speech was able to continue during stimulation but was dysarthric, and/or associated with involuntary movements of the face or throat. At some sites, counting was not tested, but passive stimulation without speech production induced motor movement or sensation around the orofacial regions. These sites are included as the orofacial effect.

Owing to the clinical stimulation set-up, bipolar stimulation was usually delivered through a pair of non-adjacent electrodes in the high-density grid (Fig. 7b, pentagrams). We consider these two electrodes together with the electrode in between as a stimulation site (Fig. 7b, dark blue circles). To test the possibilities of motor disruption and speech inhibition, we consider production activity as serving the function of motor articulation, activity prior to speech onset ('pre-speech' activity, the same as the go activity in the speech stopping task) to be potentially correlated with the function of speech motor planning, and stop activity as serving the inhibitory function. For production activity, we restricted analysis to electrodes with sustained activity (that is, showing activation throughout the duration of production). The reason for this is that if neural activity related to production only occurs at the beginning of speech production, when stimulation started, there would be no activity to be interrupted. We first plotted the speech arrest sites on the lateral side ($N = 7$ sites, 21 electrodes from five participants) on top of a combined activation map of the three types of activity on the average brain (Fig. 7c, left panel). A majority of these sites were located in the precentral gyrus, with an additional few in the IFG, consistent with the location of the speech arrest sites ($N = 36$ sites from 20 participants) found in a separate, larger dataset obtained during intra-operative mapping ($N = 34$ participants in total; Extended Data Fig. 8b, top panel). Although speech arrest sites seemed to localize to areas with stop activity (Extended Data Fig. 8a, top left panel), production and pre-speech activity also existed in nearby areas (Extended Data Fig. 8a, top middle and top right panels), forming a mixture of activity types (Fig. 7c, left panel). The location of speech error/orofacial effect sites ($N = 49$ sites, 147 electrodes from eight participants) is generally within the precentral gyrus and the

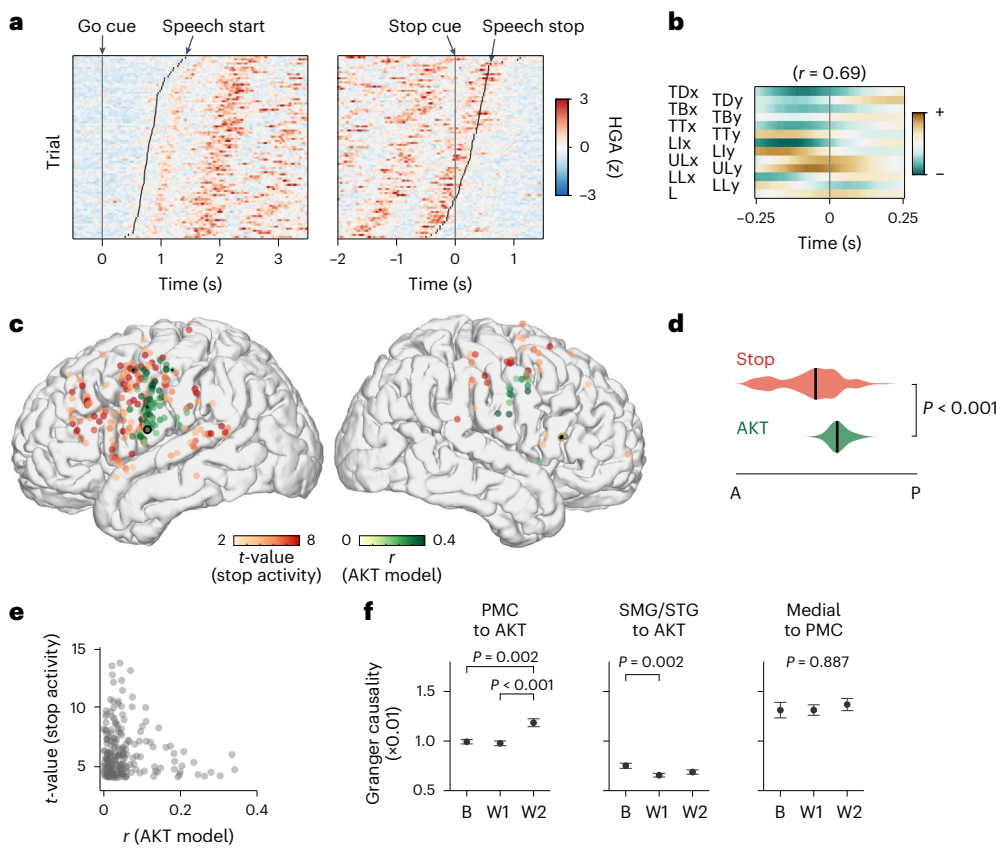


Fig. 5 | Distinct spatial localization of stop activity compared to articulatory activity. **a**, Single-trial activity of an example electrode showing strong encoding of AKT, that is, how each articulator moves during speech. Left, trials are time-aligned to the go cue, sorted by speech start. Right, time-aligned to the stop cue. The location of this electrode is indicated by a black circle in **c**. **b**, Temporal filter weight of this electrode for AKT features. The correlation coefficient r is indicated above the plot. TD, tongue dorsum; TB, tongue body; TT, tongue tip; LI, lower incisor; UL, upper lip; LL, lower lip; L, larynx. **c**, Spatial location of electrodes showing strong encoding of AKT features ($r > 0.2$, green colour) and stop electrodes (red colour). Small black dots indicate electrodes that showed strong AKT-encoding and were, at the same time, one of the stop electrodes (Extended Data Fig. 6). **d**, Distribution of electrode location of the stop and AKT-encoding electrodes along the anterior–posterior axis (only LH electrodes within the frontal areas and the postcentral gyrus are included; see **c**, left panel). A, anterior; P, posterior. Short black bar, median. The overall location of stop

electrodes was anterior to that of the AKT-encoding electrodes ($P < 0.001$, two-sided rank-sum test). **e**, Comparison of the magnitude of stop activity and the correlation coefficient (r) of the AKT-encoding model for each stop electrode. **f**, Granger causality between groups of stop electrodes and AKT-encoding electrodes (mean \pm s.e.m.), measured before and after the stop cue. PMC, stop electrodes in the lateral premotor cortex, including the precentral gyrus, IFG and MFG ($N = 125$ electrodes). AKT, AKT-encoding electrodes without stop activity ($N = 99$ electrodes). SMG/STG, stop electrodes in the supramarginal gyrus and the superior temporal gyrus ($N = 38$ electrodes). Medial, stop electrodes in medial cortical regions ($N = 7$ electrodes). B, baseline window $[-0.5, 0]$ s; W1, window 1 $[0, 0.5]$ s; W2, window 2 $[0.5, 1]$ s. Significant differences were found between a subset of windows (adjusted $P = 0.002, 1.7 \times 10^{-4}$ and 0.002 for B–W2 comparison, W1–W2 comparison in the left panel and B–W1 comparison in the middle panel; repeated measures ANOVA, post hoc analysis using paired two-sided t -test with Bonferroni corrections).

postcentral gyrus (Fig. 7c, right panel), largely overlapping with production activity (Extended Data Fig. 8a, bottom right). On the medial side, the two types of stimulation effect were also found, although the location of the three types of neural activity appears more distributed (Extended Data Fig. 8c,d).

To delineate which type of neural activity contributes to the stimulation effect, we fitted mixed-effect logistic regression models based on data from individual participants to predict stimulation results (Fig. 7d). For each stimulated electrode, the three types of activity found within 6 mm of distance were used as predictors⁵⁴ (Methods). Two separate models were built for the two types of stimulation effect (Supplementary Tables 1 and 2). We excluded electrodes from temporal regions because stop activity was primarily observed in the frontal regions, and production activity in the temporal regions was probably related to sensory processes. We grouped the speech arrest sites on the lateral cortex into two clusters according to a recent study⁴⁹. One cluster centred on the middle precentral gyrus, and another on the ventral precentral gyrus (Fig. 7c, left panel). For the middle cluster, we

found that stop activity was the only type that had a significant effect on predicting speech arrest (fixed effect: $\beta_{\text{Stop}} = 0.54, t(209) = 4.16, P < 0.001$, two-sided t -test, 95% confidence interval (CI) = [0.28, 0.79]; $\beta_{\text{Pre-speech}} = -0.11, t(209) = -0.75, P = 0.452$, two-sided t -test, 95% CI = [-0.41, 0.18]; $\beta_{\text{Production}} = 0.11, t(209) = 1.00, P = 0.317$, two-sided t -test, 95% CI = [-0.11, 0.33]; Fig. 7d), whereas production activity was the only type that had a significant effect on predicting speech error/orofacial effect (fixed effect: $\beta_{\text{Stop}} = 0.31, t(209) = 1.78, P = 0.078$, two-sided t -test, 95% CI = [-0.03, 0.65]; $\beta_{\text{Pre-speech}} = 0.44, t(209) = 1.25, P = 0.212$, two-sided t -test, 95% CI = [-0.25, 1.12]; $\beta_{\text{Production}} = 1.19, t(209) = 4.61, P < 0.001$, two-sided t -test, 95% CI = [0.68, 1.70], Fig. 7d). For the ventral cluster, none of the three types of activity had a significant effect on speech arrest. The production activity is the only type that had a significant effect on speech error/orofacial effect (fixed effect: $\beta_{\text{Stop}} = -0.18, t(127) = -0.86, P = 0.390$, two-sided t -test, 95% CI = [-0.59, 0.23]; $\beta_{\text{Pre-speech}} = -0.10, t(127) = -0.41, P = 0.686$, two-sided t -test, 95% CI = [-0.58, 0.38]; $\beta_{\text{Production}} = 0.46, t(127) = 4.05, P < 0.001$, two-sided t -test, 95% CI = [0.24, 0.69]; Fig. 7d). Similar relationship

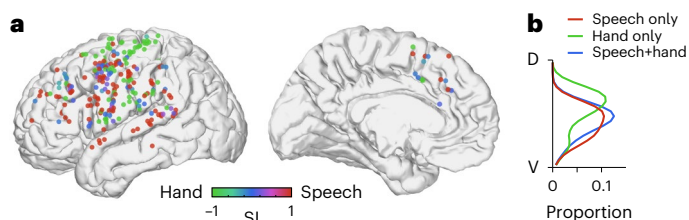


Fig. 6 | Localization of stop electrodes for speech production and hand movement. **a**, Location of stop electrodes with stop activity to ‘speech only’ (red), ‘hand only’ (green) and ‘both’ (blue). SI, selectivity index (Methods). Only LH data are included. **b**, Distribution of the location on the average brain along the dorsal–ventral (D–V) axis for the three types of electrode.

can be obtained when using alternative model calculations (Extended Data Fig. 8e). Overall, these results support that speech arrest found in clinical stimulation mapping may be caused by inhibition, rather than merely an interruption of motor execution of speech, or an interruption of pre-speech neural functions. Stimulation at regions with stop activity may induce an inhibitory behavioural effect, providing evidence for causal functions of the stop activity. The middle precentral gyrus is likely to be an important area for this inhibition⁵⁵.

Discussion

Inhibitory control of speech is critical for normal and fluent verbal communication. In this study we investigated the neural process that facilitates sudden and volitional stops during ongoing speech production. Through high-resolution neural recordings, we identified activity in the premotor cortex that was increased after the stop cue, rather than being suppressed, suggesting inhibitory functions of the premotor cortex. By comparing across task conditions and trial-by-trial variations, we found that the premotor stop activity was specific to active, volitional stopping and was absent during the natural completion of sentences. Furthermore, stop activity reflected specific components of speech stopping, including the initial response to the stop cue and execution of the stop action itself. The magnitude of activity was modulated by whether stopping occurred in the middle of a word, suggesting that inhibitory control may contain specific signals to interact with areas controlling speech articulation. Although many stop electrodes localized to the frontal and Rolandic areas, which are traditionally considered part of the speech production network, the spatial location of these electrodes was largely distinct and anterior to those encoding articulatory kinematic features. When comparing data from a hand movement stopping task, there exist cortical sites specific for speech stopping and also sites involved in both speech and hand stopping, indicating a range of inhibitory functions targeting unimodal and multimodal motor output^{56,57}. Finally, we found that electrocortical stimulation induced speech arrest, specifically in the middle precentral gyrus, showed a correlation with inhibitory control signals. These results provide new evidence to support a previously unknown function of the premotor cortex in the inhibitory control of speech.

Previous studies on the inhibitory control of action have supported the notion that the cognitive-level control of inhibition is largely confined to regions in the prefrontal cortex^{20,58–60}. Specifically, the rIFC and pre-SMA are considered the core of the cortical control of response inhibition^{23,61}. Neural activity in the rIFC activates the subthalamic nucleus through a hyperdirect pathway to achieve ‘outright’ stopping in a typical stop signal task^{24–26}. Recent work in humans using intracranial electrophysiology has confirmed the hyperdirect pathway and demonstrated that activity from the prefrontal cortex to the subthalamic nucleus mediated rapid stopping of motor outputs²⁶. Our results on early stopping of speech provide findings that are

complementary to the existing framework. First, although the spatial location of stop electrodes partially overlapped with the rIFC, stop electrodes were primarily found in premotor regions, including many along the anterior part of the precentral gyrus (Fig. 1d). Second, the neural activation occurred bilaterally, with heavy involvement of the LH. Although the difference in brain regions may be related to different task designs, for example, cancelling motor output at the initiation stage¹⁹ compared to stopping an ongoing behaviour, the LH activity is likely to be vital for immediate interaction with the speech production network on the same side. Indeed, we found that the stop activity temporally preceded the stop action, which has not been shown clearly in previous studies³⁷. Third, previous studies found pre-SMA in the medial frontal cortex has an important role in inhibitory control^{21,62,63}. Here we observed stop activity in the medial frontal cortex, although weak in amplitude, in our speech task (Fig. 1d). However, our data suggest that the activity in the lateral premotor areas did not originate from the medial side (Fig. 5f). Our results and previous studies together suggest that there may be multiple sources for inhibitory signals in the cortex, and stop activity in the premotor frontal cortex is one of them. Outside of the premotor and prefrontal regions, stop electrodes were found in scattered parietal and temporal regions. It is likely that stop activity across these brain regions forms a neural network to implement stopping. Future work is needed to investigate whether stop activity at different brain locations serves different functions, and also to map the downstream pathway of stop activity. The difference in stop activity between midword and end-of-word stopping suggests that speech inhibition may contain different commands depending on the instantaneous speech motor output and may interact with the unit of production. It is also an interesting question to probe whether aspects of stop activity are related to the ‘proactive’ stopping control described in previous studies^{36,37}.

Our results also provide an alternative view of speech arrest in clinical settings. The prevailing understanding is that speech arrest sites are ‘eloquent’, that is, indispensable nodes in the speech production network^{48,49,64–66}. Some clinicians have considered speech arrest as synonymous with Broca’s area in the IFG⁵⁰, whereas others have described it across many cortical regions with diverse mechanisms⁶⁷. Despite these views, several recent studies have demonstrated clearer localization of speech arrest to the precentral gyrus and pars opercularis (bilaterally)^{49,65,68}. It has been believed that stimulation disrupts the essential neural activity in these regions, and therefore speech can no longer be generated. Using the same electrodes in the ECoG grids, we compared the location of speech arrest sites and the neural activity for production, pre-speech functions and stopping in our study. Although we did not explicitly test for speech planning, the pre-speech activity may reflect some components of planning, together with other functions. Mixed-effect logistic regression models revealed that speech arrest sites, more specifically those in the middle precentral gyrus, were mainly associated with nearby stop activity, not production or pre-speech activity. Therefore, stimulation may activate an inhibitory pathway of speech control. The inhibition-based explanation of speech arrest has been speculated in the past^{55,69–71}. For example, negative motor areas (NMAs) were reported across perioral and premotor regions, where stimulation induced cessation of movement^{49,69,70,72}. It has been proposed that the function of NMAs may relate to inhibitory control rather than general motor programming⁷². Our results are consistent with this view. In addition, certain areas in the precentral gyrus showed stop activity for both speech and hand movement, consistent with recent studies where stimulation in precentral sites induced both speech and hand arrest^{57,73,74}. Such an effect may indicate an executive control-level function where inhibition is generally multimodal^{27,29,75}. The inhibitory mechanism provided an explanation of why speech arrest may not indicate critical functions for speech production. Although speech arrest sites can be found in the RH or SMA, lesions or resections in these regions do not

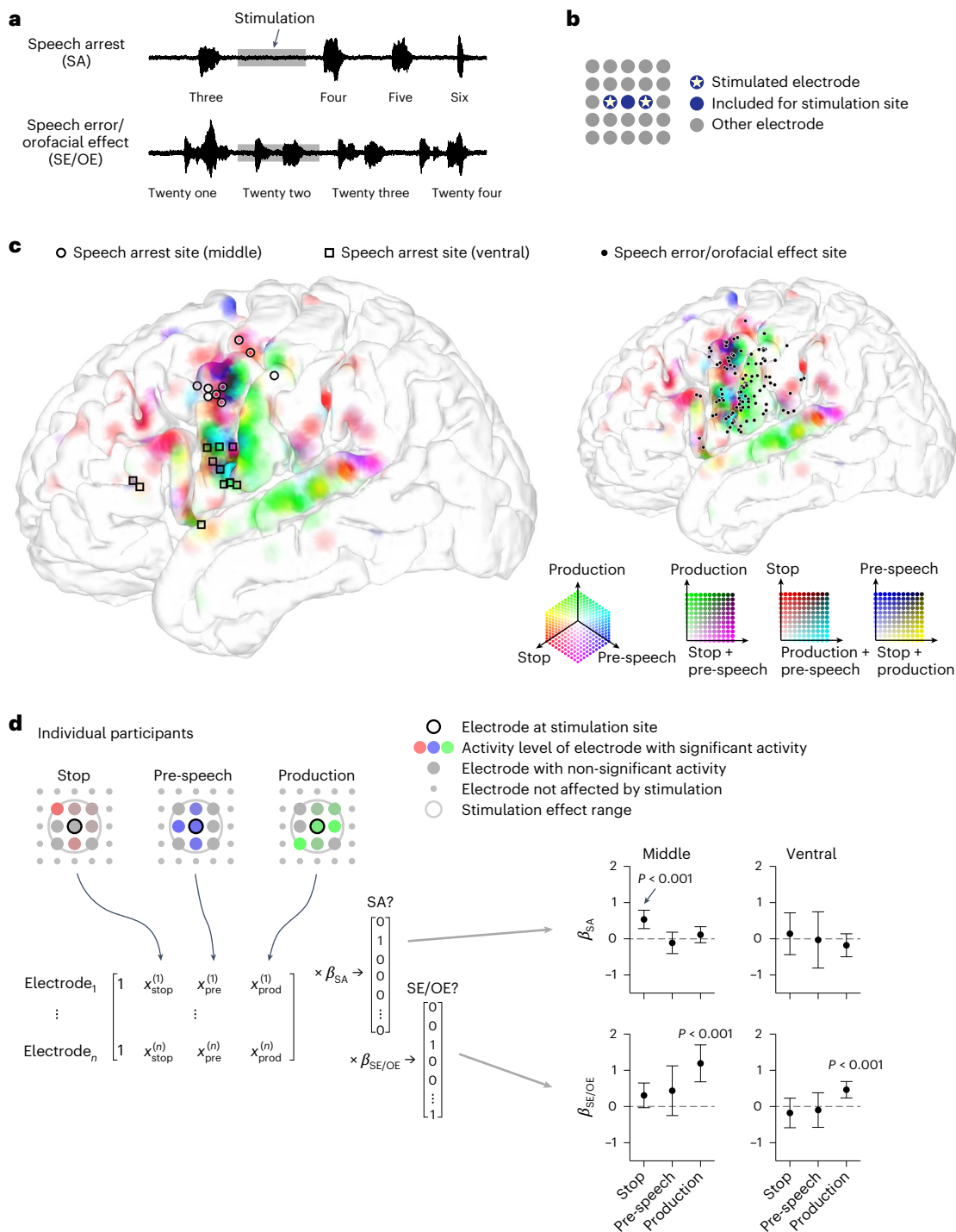


Fig. 7 | Stop activity correlates with speech arrest induced by electrocortical stimulation. **a**, Example waveforms of two stimulation effects on speech. The grey shaded region indicates the stimulation duration. **b**, Schematic of the high-density ECoG grid. Pentagrams indicate a pair of electrodes at which bipolar stimulation was delivered. Pairs are typically separated by an additional electrode owing to the configuration of the clinical stimulator. Dark blue denotes electrodes included as stimulation sites, used in **c** and **d**. **c**, Left, location of speech arrest sites overlaid on the activation map (coloured patches) generated from electrodes showing stop, pre-speech or production activity. Colour intensity indicates the magnitude of activity (based on the *t*-value). Right, location of speech error/orofacial effect sites overlaid on the same activation

map as in the left panel. **d**, Left, illustration of the mixed-effect logistic regression models to predict the stimulation effect from neural-activity patterns at neighbouring electrodes. Stop, pre-speech and production activities near each stimulated electrode were used as fixed-effect predictors. Top left, schematics showing the same stimulated electrode within the electrode grid, with the three types of neural activity illustrated separately. Colour intensity indicates the magnitude of activity. Two separate models were built for the two types of effect. SA, speech arrest; SE/OE, speech error/orofacial effect. Right, coefficients for the predictors (mean \pm 95% CI) using sites across different regions (Supplementary Tables 1 and 2 present sample sizes *N*; *P* values are provided in the Results). Middle, sites within the middle cluster. Ventral, sites within the ventral cluster.

lead to long-standing speech impairments⁷⁶. Meanwhile, anarthria or pure speech arrest is not what one would expect from disruption of speech planning; instead, paraphasias or apraxic speech would be expected. Redefining speech arrest sites as general inhibitory rather than essential for production has major clinical implications as surgical resection can be safely expanded to these sites without causing speech production deficits. A limitation of our study is that it lacks sufficient data to quantify the detailed behaviour of speech arrest. Further studies may focus on stimulation that starts in the middle of a word, potentially providing direct evidence of inhibition if the speech output is immediately cut off before the word is finished⁷⁷. It is worth noting that the relationship between speech arrest and inhibition may not be identical across different cortical regions, as the ventral cluster of speech arrest sites did not show a significant correlation to the stop activity or any of the three types of activity.

Finally, our results have important implications for models of speech production^{1,2}, particularly regarding the ventral–middle part of the precentral gyrus^{30,78} and Broca's area^{2,79,80}. Although these regions generally have facilitatory functions according to existing models, data from our study showed distinct but intermixed inhibitory functions in the same structures (Fig. 1d). Despite this spatial overlap, some interesting differences exist regarding the electrode populations associated with these two functions. At the individual electrode level, electrodes with stop activity and those with speech production-related activity did not largely overlap, indicating that the inhibitory and facilitatory functions may be separate at a smaller spatial scale than previously thought (Fig. 1f). This suggests that, instead of having separate anatomical regions for different functions, brain areas central to speech production may have mosaic subclusters of neural circuits. One possibility is that these subclusters form separate modules along the precentral gyrus that possess non-primary motor functions, in line with a recent study⁸¹. Furthermore, there is spatial segregation between electrodes showing stop activity and those encoding AKT features (Fig. 5c,d). Given our initial evidence of increased functional connectivity (Fig. 5f) and the difference in the modulation of stop activity in midword trials (Fig. 4), it is highly likely that the inhibitory function of speech interacts with articulation and planning for speech production. Future studies should aim to delineate the interaction and further elucidate the connectivity within this speech inhibition network. Our results also suggest that inhibitory control may have a more important role in normal and abnormal speech production than previously thought. In verbal communication where there is a natural, fast exchange of phrases and sentences, inhibitory signals are likely to interlace with excitatory signals with precise timing. In speech impairments such as stuttering, aberrant inhibitory signals may cause the frequent stops found in production^{9–13}.

In summary, the results we describe suggest a previously unknown mechanism for the inhibitory control of speech production. We provided a framework for a deeper understanding of the neural process underlying speech production with important implications for both basic neuroscience and clinical practice.

Methods

Participants

Thirteen participants (four male, nine female; mean \pm s.d. age, 30 ± 8 years) performed a speech stopping task and were included in the analysis. Ten of them had LH coverage and three had RH coverage. All participants were patients undergoing intracranial monitoring for intractable epilepsy. Participants were compensated for participating in the study. All procedures and protocols were approved by the Institutional Review Board of the University of California, San Francisco. Participants provided written informed consent before participating in the studies. All participants were fluent English speakers and had no cognitive deficits that could potentially affect the study. This study is registered at ClinicalTrials.gov (NCT05876910). We have complied with all relevant ethical regulations.

Task design and set-up

To test early stopping, participants performed a speech stopping task where they followed visual cues to start and stop speaking (Fig. 1a). The task was custom-programmed using Psychtoolbox-3 and MATLAB to be presented on a laptop screen (Microsoft Surface Book 2). Each trial started when a green circle (go cue) was presented at the centre of the screen and participants were instructed to start reciting the days of the week. After a random delay (2–5 s), the circle changed to red colour (stop cue), and participants were instructed to stop immediately. If 'Sunday' was reached before the stop cue was shown, participants would continue to the next cycle, starting 'Monday'. The time between the stop cue and the acoustic stop of speech is referred to as the stop reaction time (SRT). The next trial started after a short pause (2.5–3.5 s), and participants continued with recitation when the circle turned green. Throughout the trial, a cross was shown at the centre of the screen inside the coloured circle, and the participants were asked to fixate on the cross. To synchronize with neural recordings, a grey rectangle flashed at the upper right corner of the screen at the same time as the presentation of cues. A photodiode (S2281-01, Hamamatsu) was placed at the location of the rectangle on the screen and was connected to the neural recording set-up. A small number of participants recited the months of the year or counted continuously based on preference.

To compare early stopping against a natural finish condition, a subset of participants ($N = 5$ out of 13) performed a sentence reading task³⁰. In brief, participants read aloud 100 sentences from the MOCHA-TIMIT database⁸². One sentence was presented on the screen in each trial, and participants read the sentence at their own pace. There were no cues to indicate when they should stop. Each sentence was read once, so a total of 100 trials were performed.

To compare the neural activity evoked by stopping speech to stopping hand movements, a subset of participants ($N = 9$ out of 13) performed a hand movement stopping task. This task was modified from the speech stopping task with a similar presentation of cues. When the go cue was presented, participants were instructed to push a button repetitively and rhythmically using their contralateral thumb in reference to the ECoG grid. At the presentation of the stop cue, they were instructed to stop and release the button immediately. The time delay between the go cue and the stop cue was randomly jittered between 2 and 4 s.

No statistical methods were used to predetermine sample sizes, but our sample sizes are similar to or larger than those reported in previous publications^{30,78,83}.

Data acquisition and preprocessing

ECoG was acquired through subdural high-density grids (Integra or AdTech) with 1.17-mm-diameter exposed contacts and 4-mm centre-to-centre spacing. The voltage time-series signal (raw signal) from each electrode contact was amplified and digitized at a sampling rate of 3,051.7578125 Hz by a pre-amplifier (PZ5, Tucker-Davis Technologies) and processed through a digital signal processor (RZ2, Tucker-Davis Technologies). To obtain the HGA, raw signals were down-sampled to 400 Hz, notch-filtered at 60, 120 and 180 Hz to remove line noise, and Hilbert-transformed at eight logarithmically distributed bands within 70–150 Hz. Each of the eight bands was z-scored and the average was taken between bands to obtain one HGA time series. Raw signals and HGA were visually inspected to exclude bad channels and trials with artefacts. Speech audio from participants was recorded through a microphone (e845-S, Sennheiser), amplified by a microphone amplifier (MA3, Tucker-Davis Technologies) and digitized through a digital signal processor (RZ2, Tucker-Davis Technologies). The output of the push-button device (voltage signal) was digitized and recorded (RZ2, Tucker-Davis Technologies).

Electrode localization

A pre-operative MRI and a post-operative computed tomography (CT) scan were used to register the location of electrodes relative to

the brain. Reconstruction of the pial surface was performed using the pre-operative MRI image in Freesurfer. To convert the electrode coordinates from individual brains to the average brain (*cvs_avg35_inMNI152* template), we used a nonlinear surface registration in Freesurfer with a spherical sulcal-based alignment⁸⁴. This method ensures that electrodes on a given gyrus in the original participant's space remain on the same gyrus in the converted space. It does not, however, maintain the original geometry of the electrode grid.

Data analysis on stop, production and go activity

We identified the acoustic start and stop times of speech production in each trial using an energy threshold-based method. If necessary, further adjustment was made by visualizing the spectrogram of the microphone signals. To avoid the condition where participants stopped speaking by themselves independent of the stop cue, we excluded trials with an SRT less than 0.1 s (Fig. 1b and Extended Data Fig. 1a). This threshold was chosen after examining the SRTs of individual participants where no obvious and consistent cutoffs could be found in the distribution. We also excluded outlier trials with long SRTs using the 'isoutlier' function in MATLAB (Extended Data Fig. 1a). To test whether an electrode shows stop activity, we used a baseline period [−0.5, 0] s before the stop cue and an analysis period [0, 1] s after the stop cue. We set the baseline period to be during speech production because we intended to identify additional activation beyond the neural modulation caused by production. Because activity may show different delays after the stop cue across electrodes, we used a series of overlapping sliding windows of 0.2-s duration (0.1-s step size) within the analysis period. We compared the mean HGA in each of these windows with respect to the mean HGA in the baseline period and tested significance with a paired *t*-test. Significant activation was determined if the mean HGA in the sliding window was larger than that in the baseline period and if the *P* value was smaller than 0.0001. To control for multiple comparisons, we used an FDR correction for each sliding window across electrodes within each participant at a *q*-level of 0.05. An electrode was regarded as showing significant stop activity if any of the sliding windows showed significant activation. To test activity during speech production, we used a baseline period of [−0.5, 0] s before the go cue and an analysis period of [−1.5, −0.5] s before the stop cue. This analysis period covered the late part of speech production in most trials. We chose these analysis intervals to exclude electrodes that were only activated during the initial part of speech production. Applying this method allowed us to select electrodes that showed sustained activation throughout production. To compare HGA in the analysis period with that in the baseline period, we used a similar series of sliding windows as for stop activity and we followed the same steps for statistical tests. To test activity after the go cue, we used a baseline period of [−0.5, 0] s before the go cue and an analysis period of [0, t_{go}] s after the go cue. t_{go} was set for each participant separately as the 30th percentile value of the go reaction time of all trials from that participant. Trials with go reaction time shorter than t_{go} were excluded. A similar series of sliding windows were used as for stop activity, and the same statistical steps were followed. To compare the magnitude of stop activity and go activity, we used a one-sided rank-sum test. To summarize the magnitude of activity (Fig. 1d,f), we used the maximum *t*-value among the significant sliding windows. To obtain the activation map (Figs. 1d and 7c), activity magnitude from nearby electrodes was summed and mapped to the colour intensity of each vertex of the brain surface mesh.

Comparison with the natural finish condition

For each individual electrode we compared the activity at the end of speech production in the sentence reading task with the activity in the speech stopping task (Fig. 2a–d). As there was no stop cue in the sentence reading task, we used a [−0.5, 0.5]-analysis period centred at the time of speech stop. Again, we applied sliding windows of 0.2 s (0.1-step size) duration within the analysis period. We used a baseline period

[−1, −0.5] s relative to the speech stop. A similar strategy to identifying the stop activity in the speech stopping task was adopted here to test for significant activation during a natural finish. The magnitude of activation is quantified by *t*-value, which is taken from the maximum *t*-value among the significant sliding windows. To delineate whether the activity at the end of speech production is associated with regular motor activity, we divided the electrodes into two groups according to whether they have production activity in the speech stopping task, as shown in Fig. 1.

To compare the early stopping and the natural finish conditions with a similar task design, one participant performed a control task with a trial structure similar to that of the speech stopping task. The same green and red circles were used to indicate the start and stop of speech production. For each trial, the participant was instructed to say 'Monday' to 'Thursday' and then stop. If the stop cue occurred in the middle of the production, then he or she would stop immediately. The time delay of the stop cue was jittered, and the range was set such that in approximately two-thirds of the trials, the stop cue occurred after the participant had stopped. These trials were considered the natural finish condition, as there was no abrupt stopping guided by the stop cue. The activity around the time of speech stop and the stop cue (using a similar approach as the previous analysis) was compared to the early stopping condition. In addition to the control task, this participant also performed the regular speech stopping task. The one-third of trials in the control task where the stop cue occurred before the participant finished 'Thursday' and the trials in the regular speech stopping task were considered as the early stopping condition.

Temporal correlation of stop activity

To test whether stop activity in a given electrode was more correlated with the stop cue or stop action, we performed single-trial timing analyses. Because HGA in single trials is noisy, taking the maximum does not always capture the correct timing when the majority of HGA activation occurred. In the following analysis, we calculated the dominant activity time (t_d) and used it as an alternative measure of the peak time.

For stop action-related electrodes, we expect the activity to be correlated with the timing of speech stop. To identify these electrodes, we first aligned each trial to speech stop and calculated the average HGA. Our assumption is if the activity is time-locked to speech stop, then the average HGA should reflect the dominant activity in each trial. For each electrode, we performed a cross-correlation between the average HGA and each single-trial HGA, and identified the peak of the cross-correlation. The time lag of this peak (t_c) indicates how much time offset there is between the peak of the average HGA and the dominant activity of a single trial. We then used a threshold to include trials with reasonably large peaks in the cross-correlation. This threshold was set at the 95th percentile of the magnitude of all cross-correlation results (across all analysed time lags). Only trials with cross-correlation peak magnitude higher than this threshold were included and were assigned with the dominant activity time. Dominant activity time was calculated based on the time lag of the peak in the cross-correlation (t_c) and the peak time of the average HGA (t_a) relative to speech stop. For example, if the peak in the cross-correlation occurs at time lag zero, then the dominant activity time equals the peak time of the average HGA. Because the average HGA is aligned to speech stop, we convert the dominant activity time to be relative to the stop cue using each trial's SRT. Therefore, for each included trial, $t_d = t_c + t_a + \text{SRT}$. t_a is the same across trials, whereas t_c and SRT are trial-specific. We then fit linear and quadratic models between the dominant activity time and the stop reaction time (the linear model is equivalent to Pearson correlation). If either model fit showed significance ($P < 0.05$) and if the correlation coefficient was positive for the linear model, then this electrode was determined as a stop action-related electrode.

To identify cue-related electrodes, we first aligned the trials to the stop cue and obtained the averaged HGA. We then calculated the

dominant activity time using cross-correlation, similar to the previously explained technique for stop action-related electrodes. In this case, the dominant activity time is $t_d = t_c + t_s$, because the average HGA is aligned to the stop cue already. If the standard deviation of the dominant activity time is smaller than 0.15 s, and the electrode is not stop action-related, then it is determined to be a cue-related electrode. Electrodes not meeting the criteria for either type of alignment were assigned the label of ‘other’.

To quantify the activation start time relative to the time of speech stop (Fig. 3f), we aligned the HGA to the speech stop and used sliding windows (0.2-s duration, 0.1-s step size) within a [−0.5, 0.5]-s period centred at speech stop. Similar to the previously described methodology, we tested whether each of these windows had a significant increase in HGA compared to the baseline period ([−0.5, 0] s relative to the stop cue). We used the centre of the window that had the earliest significant activation ($P < 0.05$ for paired two-sided t -test) as the activation start time. Multiple comparisons were controlled by an FDR correction for each sliding window across electrodes within each participant at a q -level of 0.05.

Low-frequency activity

Beta-band activity was used to compare early stopping and natural finish conditions. To extract beta-band activity, the raw signal from each electrode was first notch-filtered to remove line noise and then zero-phased-filtered (using the ‘filtfilt’ function in MATLAB) between 20 and 30 Hz. The analytic amplitude of the signal was next computed by taking the Hilbert transform on the filtered data. The analytic amplitude was then z-scored using periods of silence as the baseline. This analytic amplitude was used for the remainder of the analyses. To test if an electrode had a significant increase in beta-band activity during stopping, we compared the mean amplitude in an analysis window [0, 0.5] s relative to the time of speech stop to that in a baseline window [−0.5, 0] s relative to the stop cue. Such intervals were chosen based on previous studies on beta suppression during motor actions^{85,86}. Significance was determined using a paired two-sided t -test with FDR correction at a q -level of 0.05.

Comparison between midword and end-of-word trials

We labelled the production in each trial for whether the ending word was completed. If speech stopped before finishing the entire word, the trial was labelled as a midword trial. Otherwise, it was labelled as an end-of-word trial. We only included electrodes with stop activity but no production activity to avoid potential confounding from signals reflecting any specific modulation to articulators during stopping. We compared the average HGA aligned to the speech stop between the two types of trial using a cluster-based permutation rank-sum test. We used $N = 1,000$ permutations and a total of one cluster as parameters. The cluster-based permutation test corrected for multiple comparisons when performing timepoint-by-timepoint comparisons between the two types of trial. To visualize the size of the stop type effect (Fig. 4c), we took the largest z-value of the rank-sum test within the significant cluster of each electrode. To characterize when the activity started to show the difference between the two stop types, we used the earliest timepoint in the significant cluster.

For the population analysis, we built a linear classifier for each participant to predict whether a single trial was a midword or end-of-word trial. Specifically, we used the average HGA within a 0.2-s window centred at speech stop from all stop electrodes without production activity. We used an L1-regularized logistic regression for the classifier. We performed 500 repeats, each time randomly picking 70% data as the training set (30% as the testing set), to obtain the mean and 95% CI of the performance. We used the area under the receiver operating characteristic (ROC) curve (AUC) to quantify the classifier performance.

Encoding of AKT

We followed similar steps as described previously³⁰ to fit the AKT-encoding model for the frontal and parietal electrodes using a total

of 13 features. We used an acoustic-to-articulatory inversion (AAI) algorithm⁸⁷ to obtain the x and y coordinates of six vocal tract points during speaking. These vocal tract points included the tongue dorsum, tongue body, tongue tip, lower incisor, upper lip and lower lip. We also included the fundamental frequency (F0) which represented the laryngeal feature. F0 was calculated using the ‘pitch’ function in MATLAB on voiced phonemes. In the other part of the speech, F0 was set to zero. HGA of each electrode was fit with a linear encoding model that predicted the HGA as the convolution of articulator kinematics (13 dimensions) with a temporal filter (Fig. 5b). We chose a filter width of 0.5 s, given results from the previous study³⁰. The model was fit using ridge regression on a training set composed of 80% of the data. The ridge parameter was evaluated with a 20-way bootstrap procedure based on the training set for each electrode. The final ridge parameter was chosen as the optimal value using the average across all electrodes. Pearson’s correlation coefficient r , calculated between the model predicted activity and the actual HGA, was used to evaluate the model fit based on a testing set composed of the remaining 20% of the data. Electrodes with a strong encoding of AKT features were determined as those with $r > 0.2$.

Granger causality

To quantify the functional connectivity between brain regions, we calculated the Granger causality (GC) for pairs of electrodes using the MVGC toolbox⁸⁸. Raw signals were first notch-filtered to remove line noise and then used in the GC analysis. We used the autoregressive integrated moving average (ARIMA) model to pre-whiten the signal to meet the stationarity requirement⁸⁹. A Kwiatkowski–Phillips–Schmidt–Shin (KPSS) test was then applied to confirm the signal was stationary. We computed GC in the frequency domain between each electrode pair from target regions. We took the maximum GC across the frequency spectrum as the GC between the electrode pair. To test whether an electrode pair had significant functional connectivity, we shuffled data across trials and calculated GC on the shuffled data to obtain a ‘null distribution’ ($N = 500$ permutations). Electrode pairs with GC values within or larger than the top 0.2% of the null distribution were considered significant and included in the analysis. We repeated the calculation in three time windows: a baseline window [−0.5, 0] s relative to the stop cue, and window 1 [0, 0.5] s and window 2 [0.5, 1] s relative to the stop cue. To compare whether there was a change in GC across electrode pairs between brain regions, we plotted the mean and standard error of all significant electrode pairs across the three windows. We used repeated measures ANOVA with post hoc analysis to find a significant change in GC between the windows ($P < 0.05$). To test whether midword and end-of-word trials showed a difference in functional connectivity, we restricted the calculation of GC on midword trials and on end-of-word trials, respectively, using the participants with enough midword trials.

Stopping of hand movement

We excluded all trials where hand stopping occurred before the stop cue. We followed the same sliding window-based strategy as in the speech stopping task to identify the stop activity and the activity during hand movement. For each electrode, we compared the stop activity between the speech and hand movement tasks. We defined a selectivity index as $(t_{\text{speech}} - t_{\text{hand}})/(t_{\text{speech}} + t_{\text{hand}})$, where t_{speech} is the t -value of the stop activity for speech and t_{hand} is the t -value of the stop activity for hand movement. If there was no significant stop activity for either modality, the corresponding t -value was set to zero. This index normalized the difference of activity to a range of [−1, 1]. A selectivity index of +1 indicated that the electrode only showed stop activity in speech, and a selectivity index of −1 indicated that the electrode only showed stop activity in hand movement.

Electrocortical stimulation and speech arrest

Participants underwent electrocortical stimulation (ECS) as part of the clinical procedures to map functional areas critical for sensorimotor

and language processing. This procedure provided an opportunity to compare the recorded neural activity (for example, stop activity) during tasks with stimulation effects using the same electrodes. Bipolar current stimulation was delivered through a pair of electrodes by a clinical stimulator (Nicolet Cortical Stimulator, Natus Medical Incorporated; Fig. 7b). We used stimulation current characterized by a biphasic pulse train, typically with 50-Hz frequency, 2-s duration and 2–6-mA amplitude. Participants were instructed to count continuously or recite the days of the week, and stimulation was delivered during this ongoing process. The amplitude of the current was first set to be 2 mA and gradually increased to probe whether stimulation affected speech production, induced sensation or generated motor output. Speech arrest sites were tested multiple times to confirm the findings.

The calculation of stop activity and production activity was performed in the same way as previously described. The pre-speech activity is the activity between the go cue and speech production onset. Here, we used the same go activity as described before. To delineate which neural function is most likely to be associated with the stimulation effect, we fit linear mixed-effect logistic regression models to predict whether stimulation at a single electrode induced an effect being tested, using the ‘fitglme’ function in MATLAB. We built two separate models to test speech arrest and speech error/orofacial effect, respectively. Stimulated electrodes within certain anatomical regions, regardless of effect, were included in the models. When calculating each type of neural activity (stop, pre-speech and production activity), electrodes were included if they showed this type of activity, regardless of whether they showed activity of other types. The same set of electrodes were used for the two models. In the speech arrest model, the outcome was 1 if there was speech arrest induced. The outcome was 0 if there was speech error/orofacial effect, other non-speech or orofacial effect (for example, limb movements) or no effect. In the speech error/orofacial effect model, the outcome was 1 if there was a speech error or orofacial effect induced, and 0 otherwise. We used the three types of neural activity (stop, pre-speech and production activity) as fixed effects and the participant ID as a random effect. For each type of neural activity at each stimulated electrode, we averaged the activity *t*-value of that type across electrodes surrounding it within a radius of 6 mm (that is, nine electrodes total). If an electrode showed significant activity, the actual *t*-value was kept and used. If an electrode did not show significant activity, the *t*-value was set to zero for the averaging. Significance in model coefficients was used to suggest the contribution of the corresponding neural function to the stimulation effect. To ensure that the significance of neural activity did not bias the model results, we also fit the models using the averaged activity *t*-value without setting the *t*-value of non-significant electrodes to zero. In this case, we excluded a few electrodes that did not pass FDR correction, to avoid being contaminated by the large *t*-values of these electrodes. For the middle and ventral clusters, we fit separate models using stimulation sites within each of the two regions, respectively. For the two-dimensional (2D) density map (Extended Data Fig. 8a–c), the location of electrodes was projected onto the anterior–posterior and dorsal–ventral axes. The 2D heatmap showing the electrode density was then overlaid on the 3D brain mesh.

For an independent cohort of patients, we performed ECS during intra-operative mapping. These patients underwent ECS to identify essential sensory, motor and language sites located in the lateral portion of the LH. ECS took place after craniotomy, during which patients were gradually awakened by reducing their sedation. Stimulation was performed using a clinical stimulator (Ojemann Cortical Stimulator, Integra LifeSciences) with typical settings (60 Hz, bipolar, biphasic, 1-ms pulse width). The stimulation threshold (range = 1.5–4.5 mA) was titrated on a per-patient basis to achieve the maximum possible stimulation current without causing after-discharges as determined by intra-operative ECoG. Patients were instructed to count slowly from 1 to 30 or recite the days of the week or months of the year. Stimulation

was administered by the surgeon during the counting or recitation process. When stimulation was found to disrupt speech at a given cortical site, the site was stimulated non-consecutively at least two more times, although the error replication protocol varied for a minority of patients. During ECS, the surgeon typically demarcated the locations of sensory, motor and language sites with sterile paper tags. ECS mapping was video-recorded (including capturing both the exposed brain and, with a second camera, the patient’s face) for later neuroanatomical co-registration and behavioural analysis. During data analysis, these videos were annotated to identify precise neuroanatomical loci on a given patient’s brain for each stimulation site. The stereotactic coordinates and gross anatomical region of interest for each stimulation site were recorded and registered as coordinates on a standardized, average brain using a custom MATLAB script by a trained neurologist blinded to the stimulation effect observed at each site.

Reporting summary

Further information on research design is available in the Nature Portfolio Reporting Summary linked to this Article.

Data availability

The data that support the main findings of this study are available via Zenodo⁹⁰ at <https://doi.org/10.5281/zenodo.1451260>. Raw data are available from the corresponding author upon request.

Code availability

The code used for data analysis in this study is available via Zenodo⁹¹ at <https://doi.org/10.5281/zenodo.14513144>.

References

1. Guenther, F. H. *Neural Control of Speech* (MIT Press, 2016); <https://doi.org/10.7551/mitpress/10471.001.0001>
2. Hickok, G. Computational neuroanatomy of speech production. *Nat. Rev. Neurosci.* **13**, 135–145 (2012).
3. Houde, J. F. & Nagarajan, S. S. Speech production as state feedback control. *Front. Hum. Neurosci.* **5**, 82 (2011).
4. Ladefoged, P., Silverstein, R. & Papçun, G. Interruptibility of speech. *J. Acoust. Soc. Am.* **54**, 1105–1108 (1973).
5. Tilsen, S. Effects of syllable stress on articulatory planning observed in a stop-signal experiment. *J. Phon.* **39**, 642–659 (2011).
6. Sacks, H., Schegloff, E. A. & Jefferson, G. A simplest systematics for the organization of turn-taking for conversation. *Language* **50**, 696–735 (1974).
7. Heldner, M. & Edlund, J. Pauses, gaps and overlaps in conversations. *J. Phon.* **38**, 555–568 (2010).
8. Brady, P. T. A statistical analysis of on-off patterns in 16 conversations. *Bell Syst. Tech. J.* **47**, 73–91 (1968).
9. Eggers, K., De Nil, L. F. & Van den Bergh, B. R. Temperament dimensions in stuttering and typically developing children. *J. Fluency Disord.* **35**, 355–372 (2010).
10. Markett, S. et al. Impaired motor inhibition in adults who stutter – evidence from speech-free stop-signal reaction time tasks. *Neuropsychologia* **91**, 444–450 (2016).
11. Neef, N. E. et al. Structural connectivity of right frontal hyperactive areas scales with stuttering severity. *Brain* **141**, 191–204 (2018).
12. Orpella, J. et al. Reactive inhibitory control precedes overt stuttering events. *Neurobiol. Lang.* **5**, 432–453 (2024).
13. Chang, S. E. & Guenther, F. H. Involvement of the cortico-basal ganglia-thalamocortical loop in developmental stuttering. *Front. Psychol.* **10**, 3088 (2020).
14. Alderson, R. M., Rapport, M. D. & Kofler, M. J. Attention-deficit/hyperactivity disorder and behavioral inhibition: a meta-analytic review of the stop-signal paradigm. *J. Abnorm. Child Psychol.* **35**, 745–758 (2007).

15. Kalaska, J. F. & Crammond, D. J. Deciding not to GO: neuronal correlates of response selection in a GO/NOGO task in primate premotor and parietal cortex. *Cereb. Cortex* **5**, 410–428 (1995).
16. Aron, A. R. The neural basis of inhibition in cognitive control. *Neuroscientist* **13**, 214–228 (2007).
17. Fu, Z., Sajad, A., Errington, S. P., Schall, J. D. & Rutishauser, U. Neurophysiological mechanisms of error monitoring in human and non-human primates. *Nat. Rev. Neurosci.* **24**, 153–172 (2023).
18. Bouvier, J. et al. Descending command neurons in the brainstem that halt locomotion. *Cell* **163**, 1191–1203 (2015).
19. Logan, G. D. & Cowan, W. B. On the ability to inhibit thought and action: a theory of an act of control. *Psychol. Rev.* **91**, 295–327 (1984).
20. Swann, N. et al. Intracranial EEG reveals a time- and frequency-specific role for the right inferior frontal gyrus and primary motor cortex in stopping initiated responses. *J. Neurosci.* **29**, 12675–12685 (2009).
21. Swann, N. C. et al. Roles for the pre-supplementary motor area and the right inferior frontal gyrus in stopping action: electrophysiological responses and functional and structural connectivity. *Neuroimage* **59**, 2860–2870 (2012).
22. Schaum, M. et al. Right inferior frontal gyrus implements motor inhibitory control via beta-band oscillations in humans. *eLife* **10**, e61679 (2021).
23. Aron, A. R., Robbins, T. W. & Poldrack, R. A. Inhibition and the right inferior frontal cortex: one decade on. *Trends Cogn. Sci.* **18**, 177–185 (2014).
24. Aron, A. R. & Poldrack, R. A. Cortical and subcortical contributions to stop signal response inhibition: role of the subthalamic nucleus. *J. Neurosci.* **26**, 2424–2433 (2006).
25. Aron, A. R., Behrens, T. E., Smith, S., Frank, M. J. & Poldrack, R. A. Triangulating a cognitive control network using diffusion-weighted Magnetic Resonance Imaging (MRI) and functional MRI. *J. Neurosci.* **27**, 3743–3752 (2007).
26. Chen, W. et al. Prefrontal-subthalamic hyperdirect pathway modulates movement inhibition in humans. *Neuron* **106**, 579–588.e3 (2020).
27. Cai, W., Oldenkamp, C. L. & Aron, A. R. Stopping speech suppresses the task-irrelevant hand. *Brain Lang.* **120**, 412–415 (2012).
28. Wagner, J., Wessel, J. R., Ghahremani, A. & Aron, A. R. Establishing a right frontal beta signature for stopping action in scalp EEG: implications for testing inhibitory control in other task contexts. *J. Cogn. Neurosci.* **30**, 107–118 (2018).
29. Xue, G., Aron, A. R. & Poldrack, R. A. Common neural substrates for inhibition of spoken and manual responses. *Cereb. Cortex* **18**, 1923–1932 (2008).
30. Chartier, J., Anumanchipalli, G. K., Johnson, K. & Chang, E. F. Encoding of articulatory kinematic trajectories in human speech sensorimotor cortex. *Neuron* **98**, 1042–1054.e4 (2018).
31. Duque, J., Labruna, L., Verset, S., Olivier, E. & Ivry, R. B. Dissociating the role of prefrontal and premotor cortices in controlling inhibitory mechanisms during motor preparation. *J. Neurosci.* **32**, 806–816 (2012).
32. Buch, E. R., Mars, R. B., Boorman, E. D. & Rushworth, M. F. S. A network centered on ventral premotor cortex exerts both facilitatory and inhibitory control over primary motor cortex during action reprogramming. *J. Neurosci.* **30**, 1395–1401 (2010).
33. Adam, E. M., Johns, T. & Sur, M. Dynamic control of visually guided locomotion through corticosubthalamic projections. *Cell Rep.* **40**, 111139 (2022).
34. Fonken, Y. M. et al. Frontal and motor cortex contributions to response inhibition: evidence from electrocorticography. *J. Neurophysiol.* **115**, 2224–2236 (2016).
35. Tatz, J. R., Soh, C. & Wessel, J. R. Common and unique inhibitory control signatures of action-stopping and attentional capture suggest that actions are stopped in two stages. *J. Neurosci.* **41**, 8826–8838 (2021).
36. Chikazoe, J. et al. Preparation to inhibit a response complements response inhibition during performance of a stop-signal task. *J. Neurosci.* **29**, 15870–15877 (2009).
37. Swann, N. C., Tandon, N., Pieters, T. A. & Aron, A. R. Intracranial electroencephalography reveals different temporal profiles for dorsal- and ventro-lateral prefrontal cortex in preparing to stop action. *Cereb. Cortex* **23**, 2479–2488 (2013).
38. Heinrichs-Graham, E., Kurz, M. J., Gehring, J. E. & Wilson, T. W. The functional role of post-movement beta oscillations in motor termination. *Brain Struct. Funct.* **222**, 3075–3086 (2017).
39. Zhang, R., Geng, X. & Lee, T. M. C. Large-scale functional neural network correlates of response inhibition: an fMRI meta-analysis. *Brain Struct. Funct.* **222**, 3973–3990 (2017).
40. Yeung, M. K., Tsuchida, A. & Fellows, L. K. Causal prefrontal contributions to stop-signal task performance in humans. *J. Cogn. Neurosci.* **33**, 1784–1797 (2021).
41. Mirabella, G., Pani, P. & Ferraina, S. Neural correlates of cognitive control of reaching movements in the dorsal premotor cortex of rhesus monkeys. *J. Neurophysiol.* **106**, 1454–1466 (2011).
42. Mattia, M. et al. Stop-event-related potentials from intracranial electrodes reveal a key role of premotor and motor cortices in stopping ongoing movements. *Front. Neuroeng.* **5**, 12 (2012).
43. Parmigiani, S. & Cattaneo, L. Stimulation of the dorsal premotor cortex, but not of the supplementary motor area proper, impairs the stop function in a STOP signal task. *Neuroscience* **394**, 14–22 (2018).
44. Giarrocco, F. et al. Neuronal dynamics of signal selective motor plan cancellation in the macaque dorsal premotor cortex. *Cortex* **135**, 326–340 (2021).
45. Pani, P. et al. Neuronal population dynamics during motor plan cancellation in nonhuman primates. *Proc. Natl Acad. Sci. USA* **119**, e2122395119 (2022).
46. Cardelluccio, P., Dolfini, E. & D'Ausilio, A. The role of dorsal premotor cortex in joint action stopping. *iScience* **24**, 103330 (2021).
47. Menon, V., Adleman, N. E., White, C. D., Glover, G. H. & Reiss, A. L. Error-related brain activation during a Go/NoGo response inhibition task. *Hum. Brain Mapp.* **12**, 131–143 (2001).
48. Penfield, W. & Roberts, L. *Speech and Brain Mechanisms* (Princeton Univ. Press, 1959).
49. Lu, J. et al. Functional maps of direct electrical stimulation-induced speech arrest and anomia: a multicentre retrospective study. *Brain* **144**, 2541–2553 (2021).
50. Quiñones-Hinojosa, A., Ojemann, S. G., Sanai, N., Dillon, W. P. & Berger, M. S. Preoperative correlation of intraoperative cortical mapping with magnetic resonance imaging landmarks to predict localization of the Broca area. *J. Neurosurg.* **99**, 311–318 (2003).
51. Brannen, J. H. et al. Reliability of functional MR imaging with word-generation tasks for mapping Broca's area. *Am. J. Neuroradiol.* **22**, 1711–1718 (2001).
52. Fitzgerald, D. B. et al. Location of language in the cortex: a comparison between functional MR imaging and electrocortical stimulation. *Am. J. Neuroradiol.* **18**, 1529–1539 (1997).
53. Ojemann, G. A. Brain organization for language from the perspective of electrical stimulation mapping. *Behav. Brain Sci.* **6**, 189–206 (1983).
54. Muller, L. et al. Direct electrical stimulation of human cortex evokes high gamma activity that predicts conscious somatosensory perception. *J. Neural Eng.* **15**, 026015 (2018).

55. Silva, A. B. et al. A neurosurgical functional dissection of the middle precentral gyrus during speech production. *J. Neurosci.* **42**, 8416–8426 (2022).
56. Gavrilov, N. & Nieder, A. Distinct neural networks for the volitional control of vocal and manual actions in the monkey homologue of Broca's area. *eLife* **10**, e62797 (2021).
57. Breshears, J. D., Southwell, D. G. & Chang, E. F. Inhibition of manual movements at speech arrest sites in the posterior inferior frontal lobe. *Clin. Neurosurg.* **85**, E496–E501 (2019).
58. Bari, A. & Robbins, T. W. Inhibition and impulsivity: behavioral and neural basis of response control. *Prog. Neurobiol.* **108**, 44–79 (2013).
59. Rubia, K., Smith, A. B., Brammer, M. J. & Taylor, E. Right inferior prefrontal cortex mediates response inhibition while mesial prefrontal cortex is responsible for error detection. *Neuroimage* **20**, 351–358 (2003).
60. Wessel, J. R., Conner, C. R., Aron, A. R. & Tandon, N. Chronometric electrical stimulation of right inferior frontal cortex increases motor braking. *J. Neurosci.* **33**, 19611–19619 (2013).
61. Aron, A. R., Robbins, T. W. & Poldrack, R. A. Inhibition and the right inferior frontal cortex. *Trends Cogn. Sci.* **8**, 170–177 (2004).
62. Chen, X., Scangos, K. W. & Stuphorn, V. Supplementary motor area exerts proactive and reactive control of arm movements. *J. Neurosci.* **30**, 14657–14675 (2010).
63. Chao, H. H. A., Luo, X., Chang, J. L. K. & Li, C. S. R. Activation of the pre-supplementary motor area but not inferior prefrontal cortex in association with short stop signal reaction time—an intra-subject analysis. *BMC Neurosci.* **10**, 75 (2009).
64. Ojemann, G., Ojemann, J., Lettich, E. & Berger, M. Cortical language localization in left, dominant hemisphere: an electrical stimulation mapping investigation in 117 patients. *J. Neurosurg.* **71**, 316–326 (1989).
65. Tate, M. C., Herbet, G., Moritz-Gasser, S., Tate, J. E. & Duffau, H. Probabilistic map of critical functional regions of the human cerebral cortex: Broca's area revisited. *Brain* **137**, 2773–2782 (2014).
66. Sanai, N., Mirzadeh, Z. & Berger, M. S. Functional outcome after language mapping for glioma resection. *New Engl. J. Med.* **358**, 18–27 (2008).
67. Kabakoff, H. et al. Timing and location of speech errors induced by direct cortical stimulation. *Brain Commun.* **6**, fcae053 (2024).
68. Chang, E. F. et al. Stereotactic probability and variability of speech arrest and anomia sites during stimulation mapping of the language dominant hemisphere. *J. Neurosurg.* **126**, 114–121 (2017).
69. Rech, F. et al. A probabilistic map of negative motor areas of the upper limb and face: a brain stimulation study. *Brain* **142**, 952–965 (2019).
70. Mikuni, N. et al. Evidence for a wide distribution of negative motor areas in the periolandic cortex. *Clin. Neurophysiol.* **117**, 33–40 (2006).
71. Hannah, R. & Aron, A. R. Towards real-world generalizability of a circuit for action-stopping. *Nat. Rev. Neurosci.* **22**, 538–552 (2021).
72. Filevich, E., Kühn, S. & Haggard, P. Negative motor phenomena in cortical stimulation: implications for inhibitory control of human action. *Cortex* **48**, 1251–1261 (2012).
73. Leonard, M. K. et al. Direct cortical stimulation of inferior frontal cortex disrupts both speech and music production in highly trained musicians. *Cogn. Neuropsychol.* **36**, 158–166 (2019).
74. Zhou, Y. et al. Electrical stimulation-induced speech-related negative motor responses in the lateral frontal cortex. *J. Neurosurg.* **137**, 496–504 (2022).
75. Wessel, J. R. & Aron, A. R. On the globality of motor suppression: unexpected events and their influence on behavior and cognition. *Neuron* **93**, 259–280 (2017).
76. Krainik, A. et al. Postoperative speech disorder after medial frontal surgery: role of the supplementary motor area. *Neurology* **60**, 587–594 (2003).
77. Ferpozzi, V. et al. Broca's area as a pre-articulatory phonetic encoder: gating the motor program. *Front. Hum. Neurosci.* **12**, 64 (2018).
78. Bouchard, K. E., Mesgarani, N., Johnson, K. & Chang, E. F. Functional organization of human sensorimotor cortex for speech articulation. *Nature* **495**, 327–332 (2013).
79. Long, M. A. et al. Functional segregation of cortical regions underlying speech timing and articulation. *Neuron* **89**, 1187–1193 (2016).
80. Flinker, A. et al. Redefining the role of Broca's area in speech. *Proc. Natl Acad. Sci. USA* **112**, 2871–2875 (2015).
81. Gordon, E. M. et al. A somato-cognitive action network alternates with effector regions in motor cortex. *Nature* **617**, 351–359 (2023).
82. Wrench, A. MOCHA: multichannel articulatory database <https://www.cstr.ed.ac.uk/research/projects/artic/mocha.html> (1999).
83. Castellucci, G. A., Kovach, C. K., Howard, M. A., Greenlee, J. D. W. & Long, M. A. A speech planning network for interactive language use. *Nature* **602**, 117–122 (2022).
84. Fischl, B., Sereno, M. I., Tootell, R. B. H. & Dale, A. M. High-resolution intersubject averaging and a coordinate system for the cortical surface. *Hum. Brain Mapp.* **8**, 272–284 (1999).
85. Sanes, J. N. & Donoghue, J. P. Oscillations in local field potentials of the primate motor cortex during voluntary movement. *Proc. Natl Acad. Sci. USA* **90**, 4470–4474 (1993).
86. Cassim, F. et al. Does post-movement beta synchronization reflect an idling motor cortex? *Neuroreport* **12**, 3859–3863 (2001).
87. Parrot, M., Millet, J. & Dunbar, E. Independent and automatic evaluation of speaker-independent acoustic-to-articulatory reconstruction. In *Proc. Annual Conference of the International Speech Communication Association, INTERSPEECH* 3740–3744 (ISCA, 2020).
88. Barnett, L. & Seth, A. K. The MVGC multivariate Granger causality toolbox: a new approach to Granger-causal inference. *J. Neurosci. Methods* **223**, 50–68 (2014).
89. Leuthold, A. C., Langheim, F. J. P., Lewis, S. M. & Georgopoulos, A. P. Time series analysis of magnetoencephalographic data during copying. *Exp. Brain Res.* **164**, 411–422 (2005).
90. Zhao, L., Silva, A. B., Kurteff, G. L. & Chang, E. F. Inhibitory control of speech production in the human premotor frontal cortex. *Zenodo* <https://doi.org/10.5281/zenodo.14512660> (2024).
91. Zhao, L. Inhibitory control of speech production in the human premotor frontal cortex. *Zenodo* <https://doi.org/10.5281/zenodo.14513144> (2024).

Acknowledgements

We thank P. Hullett and others for their help with electrocortical stimulation. We thank J. Rolston for the initial work on the project. We thank M. Leonard and S. Harper for their comments on the manuscript. We thank R. Ivry, J. Lu and X. Tong for helpful discussions on the results. We thank J. Kleen, N. Fox, M. Desai and A. Shafi for help with the intra-operative mapping data analysis. We thank A. Fong for technical assistance and record enquiries. We thank Y. Li and I. Norman for suggestions on statistics. This work was supported by grants from the NIH (DP2OD008627 and U01NS098971-01 to E.F.C., K99DC020235 to L.Z. and F30DC021872 to A.B.S.). This research was also supported by the New York Stem Cell Foundation, the Howard Hughes Medical Institute, the McKnight Foundation, the Shurl and Kay Curci Foundation and the William K. Bowes Foundation. The funders had no role in study design, data collection and analysis, decision to publish or preparation of the manuscript.

Author contributions

L.Z. and E.F.C. conceived the research and designed the experiment. L.Z., E.F.C. and others collected the data. L.Z., A.B.S. and G.L.K. analysed the data. L.Z., A.B.S. and E.F.C. wrote and revised the manuscript. E.F.C. supervised the project.

Competing interests

The authors declare no competing interests.

Additional information

Extended data is available for this paper at
<https://doi.org/10.1038/s41562-025-02118-4>.

Supplementary information The online version contains supplementary material available at
<https://doi.org/10.1038/s41562-025-02118-4>.

Correspondence and requests for materials should be addressed to Edward F. Chang.

Peer review information *Nature Human Behaviour* thanks

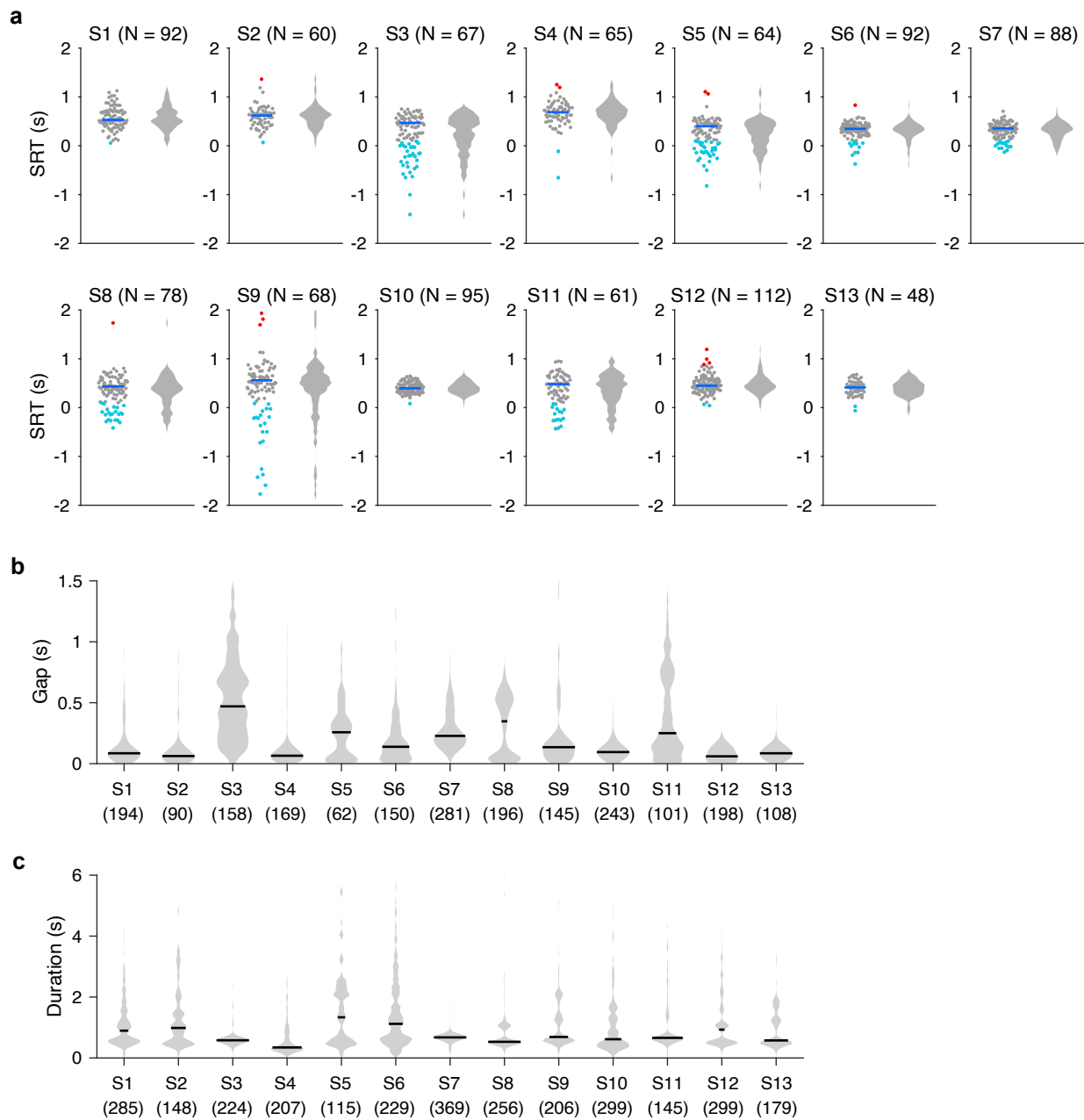
Gregory Cogan and the other, anonymous, reviewer(s) for their contribution to the peer review of this work. Peer reviewer reports are available.

Reprints and permissions information is available at
www.nature.com/reprints.

Publisher's note Springer Nature remains neutral with regard to jurisdictional claims in published maps and institutional affiliations.

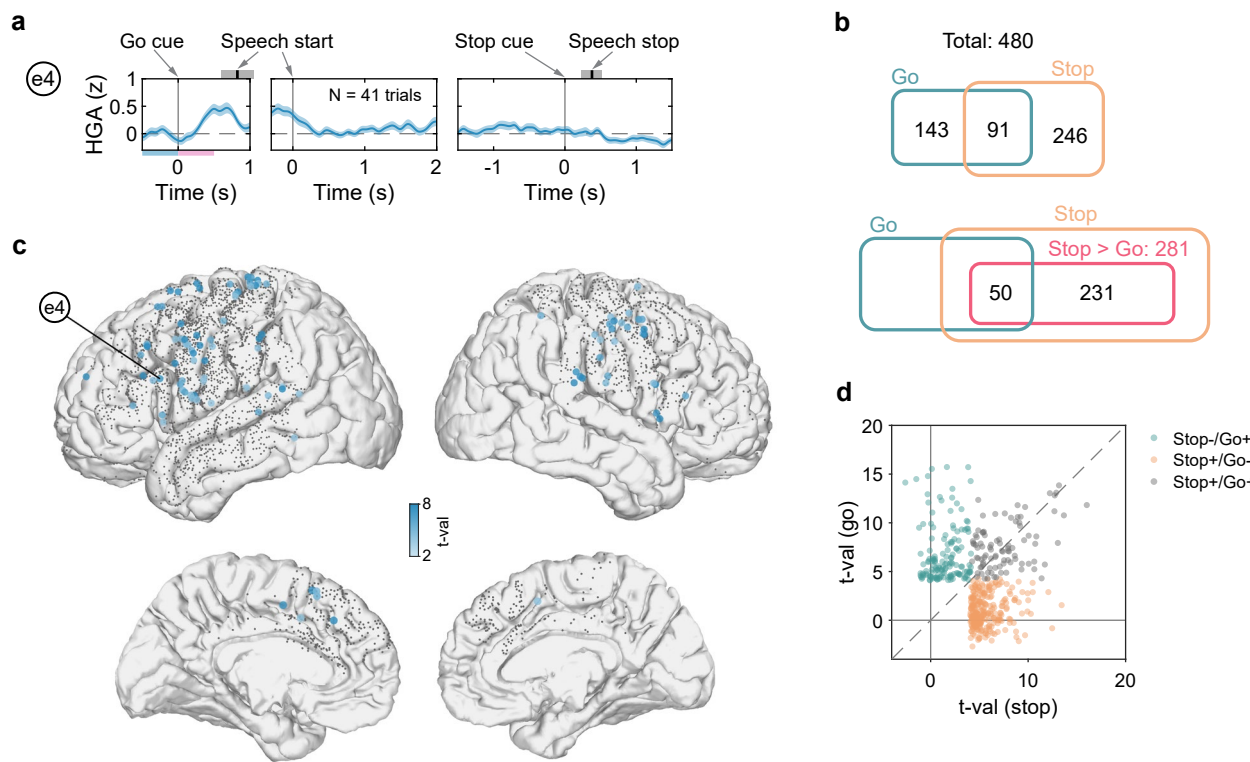
Springer Nature or its licensor (e.g. a society or other partner) holds exclusive rights to this article under a publishing agreement with the author(s) or other rightsholder(s); author self-archiving of the accepted manuscript version of this article is solely governed by the terms of such publishing agreement and applicable law.

© The Author(s), under exclusive licence to Springer Nature Limited 2025



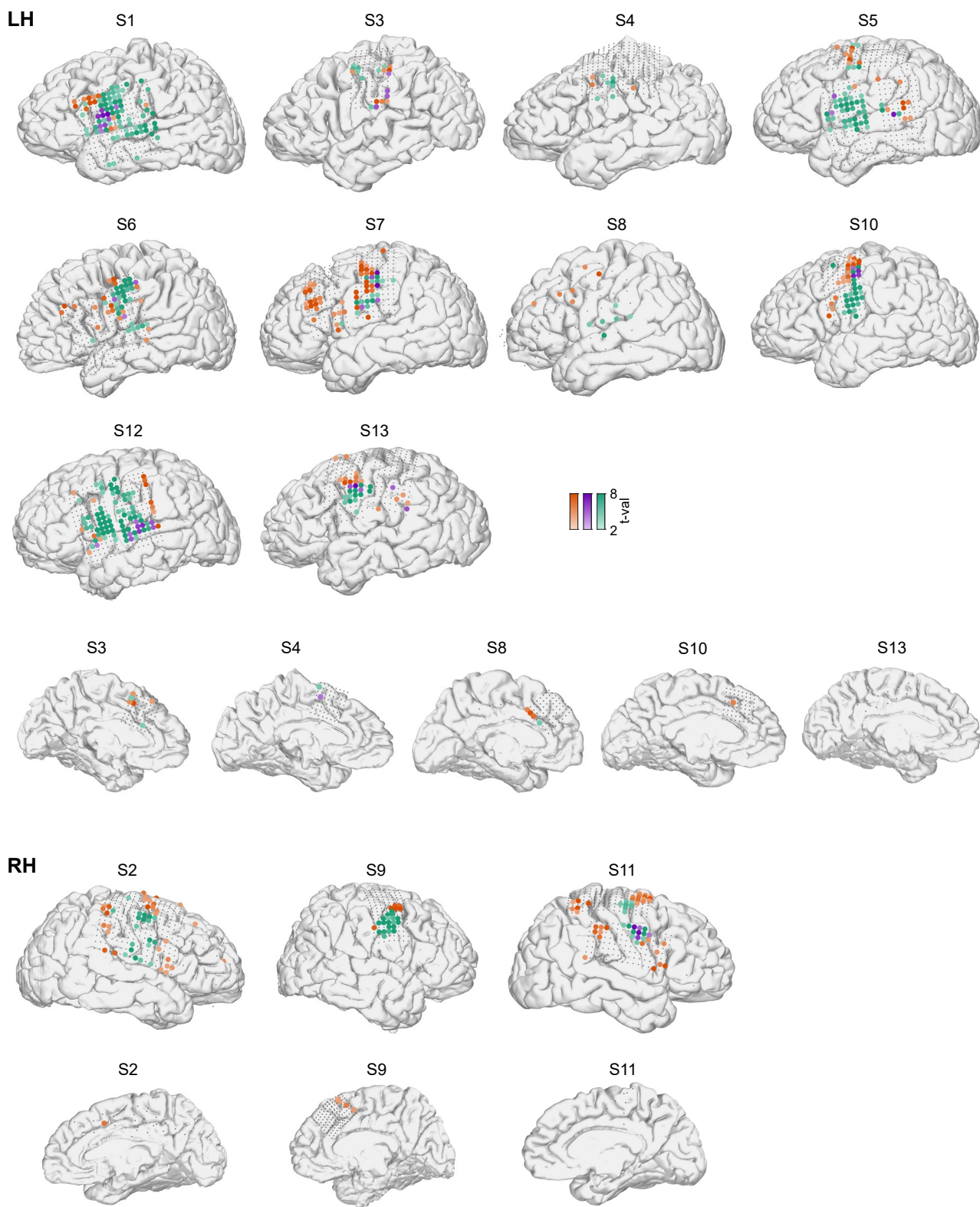
Extended Data Fig. 1 | Characteristics of speech production and stopping for individual participants. (a) Stop reaction time (SRT). In each panel, SRTs for individual trials are shown on the left, and the distribution is shown on the right. Red dots: excluded outliers with long SRT. Blue dots: excluded trials with SRT < 0.1 s. Blue horizontal bar: median SRT for included trials. The number of included trials (N) is labeled on top of each panel. (b) Distribution of the gap

time between utterances. Black horizontal bar: median. The number within the parentheses below each participant ID indicates the number of samples for that participant. (c) Distribution of the duration of utterances. Black horizontal bar: median. The number within the parentheses below each participant ID indicates the number of samples for that participant.



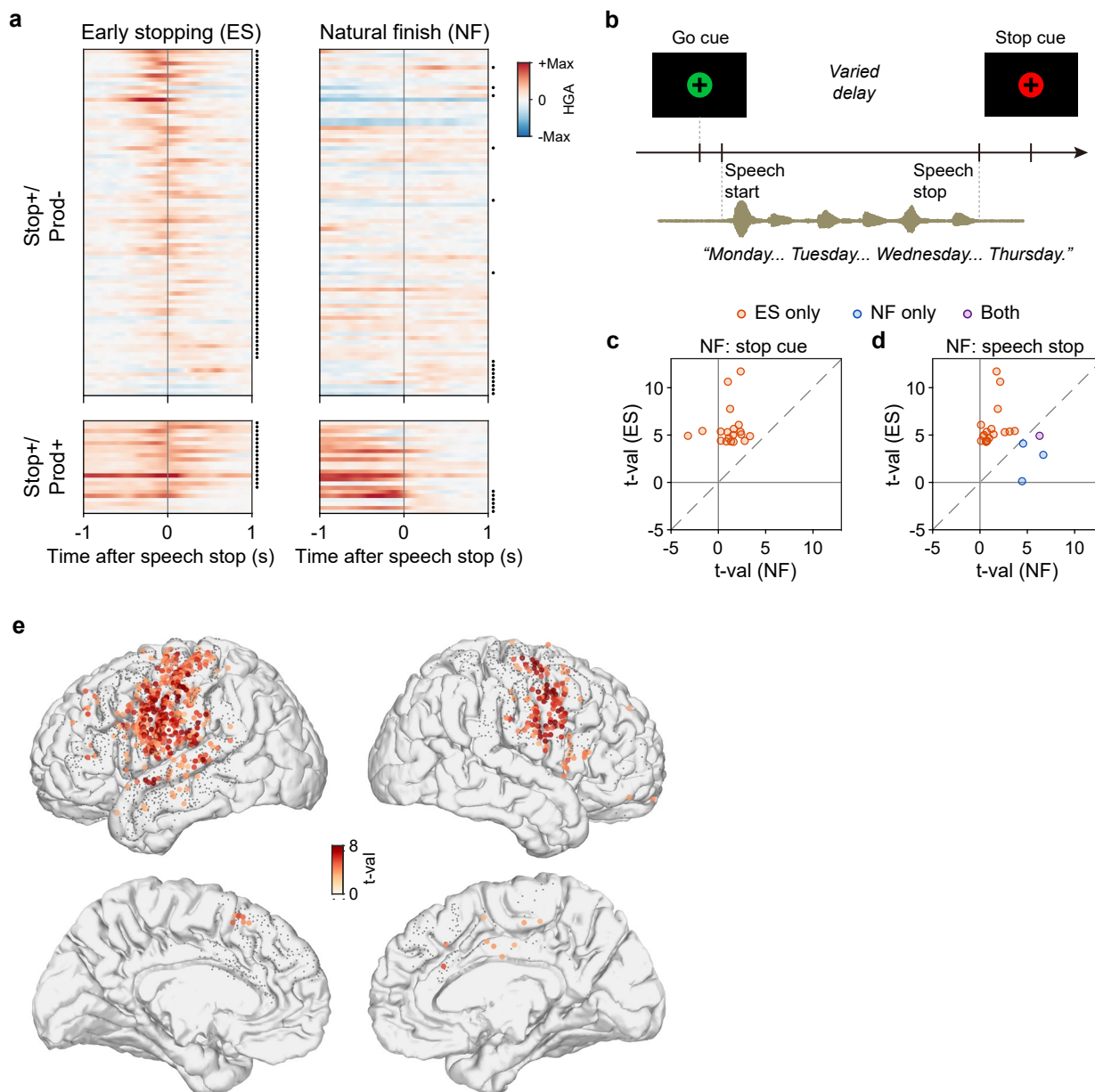
Extended Data Fig. 2 | Neural activity after the go cue. (a) Similar format as Fig. 1c. Example electrode (e4) showing increased activity (mean \pm s.e.m.) after the go cue (go activity). The location of this electrode is indicated in (c). (b) Top: Venn diagram showing the number of electrodes with go activity, stop activity, and both. Bottom: Venn diagram illustrating the number of stop electrodes (pink), defined as electrodes showing significant stop activity and their stop activity is significantly larger than the go activity. The number of stop electrodes with and without significant go activity is indicated, respectively. (c) Similar

format as Fig. 1d. Location of electrodes showing go activity, with stop electrodes and electrodes showing production activity excluded. Color intensity indicates the magnitude of activity (t-value). Gray dots indicate the electrode coverage. (d) Similar format as Fig. 1f. Scatter plot of stop and go activity magnitude, including electrodes showing significant stop or go activity. Each circle indicates a single electrode. Turquoise: electrodes showing go activity but not stop activity. Light orange: electrodes showing stop activity but not go activity. Gray: electrodes showing both types of activity.



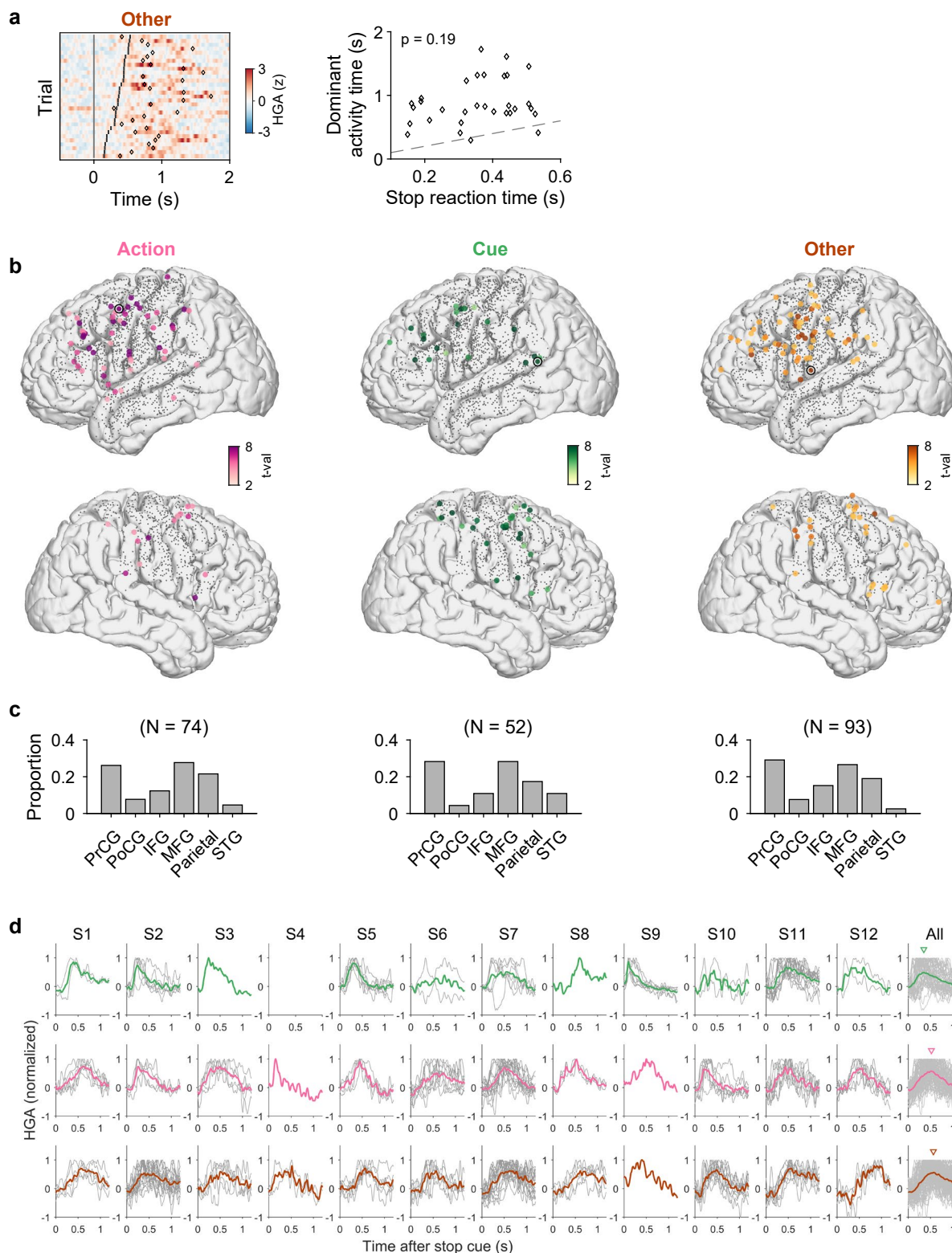
Extended Data Fig. 3 | Location of electrodes showing activation during speech production and stopping in each participant. The spatial location of stop electrodes and electrodes showing activity during production (colored circles) in each participant. Color intensity indicates the magnitude of activity

(t -value). Orange: stop electrodes with no production activity. Purple: stop electrodes with production activity. Green: electrodes with production activity, excluding stop electrodes. LH: left hemisphere. RH: right hemisphere.



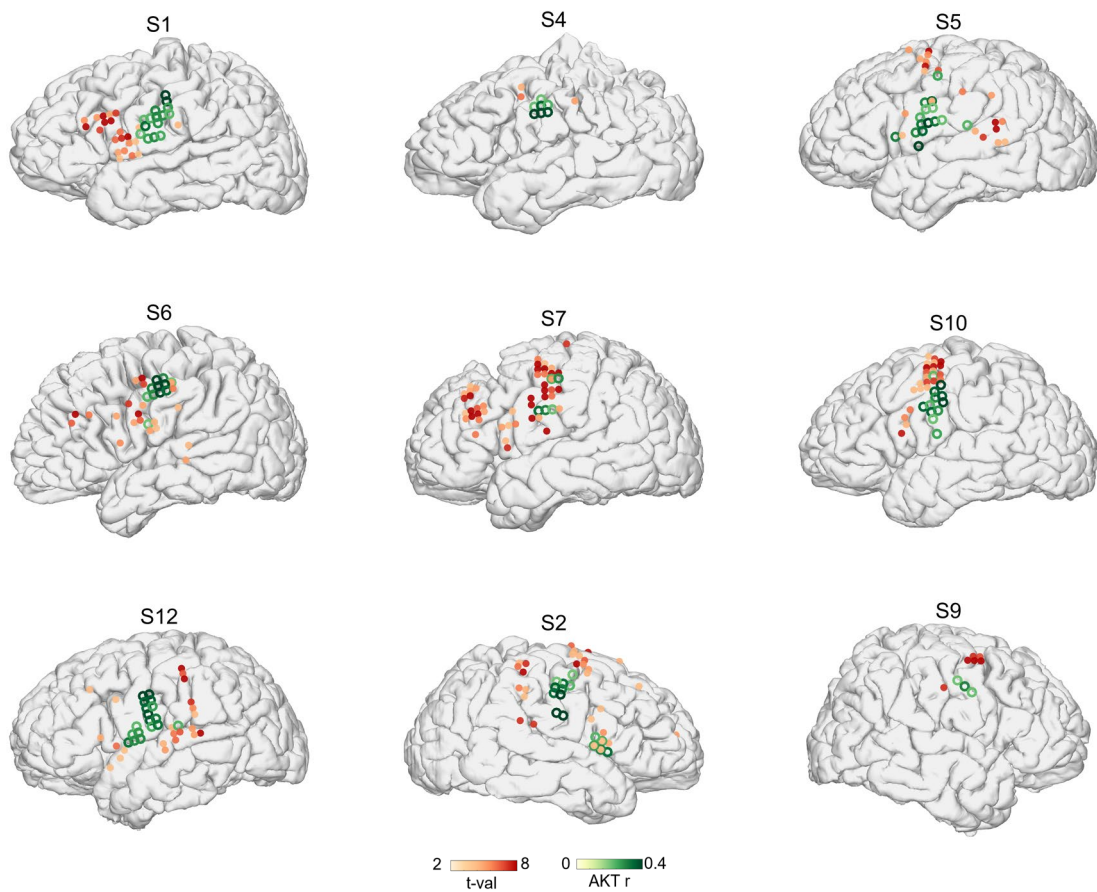
Extended Data Fig. 4 | High-gamma and low-frequency activity during early stopping and natural finish. (a) Heatmaps illustrating the averaged activity across trials for each electrode in Fig. 2b (top) and Fig. 2d (bottom). Each row indicates one individual electrode, with the same electrode order in the left and right panels. Black dots to the right of the heatmap indicate significant stop activity. (b) Schematic of the control task. The participant was instructed to say "Monday" through "Thursday" and then stop even if the green circle was still shown. In most trials, the red circle (stop cue) occurred after the participant had stopped. (c) Scatter plot of high-gamma activity magnitude (t-val) during early stopping (ES) and natural finish (NF) for all

electrodes showing stop activity in either condition (N=1 participant tested in the control task, regardless of production activity). Activity in the NF condition is aligned to the stop cue. Each marker indicates a single electrode. (d) Similar format as (c), activity in the NF condition is aligned to speech stop. (e) The spatial location of electrodes showing beta-band activation during stopping for all participants (N=12 participants in the speech stopping task, excluding S13 who mainly performed the control task). Color intensity indicates the magnitude of activity (t-value). Gray dots indicate the electrode coverage. The white circle indicates the example electrodes shown in Fig. 2e.

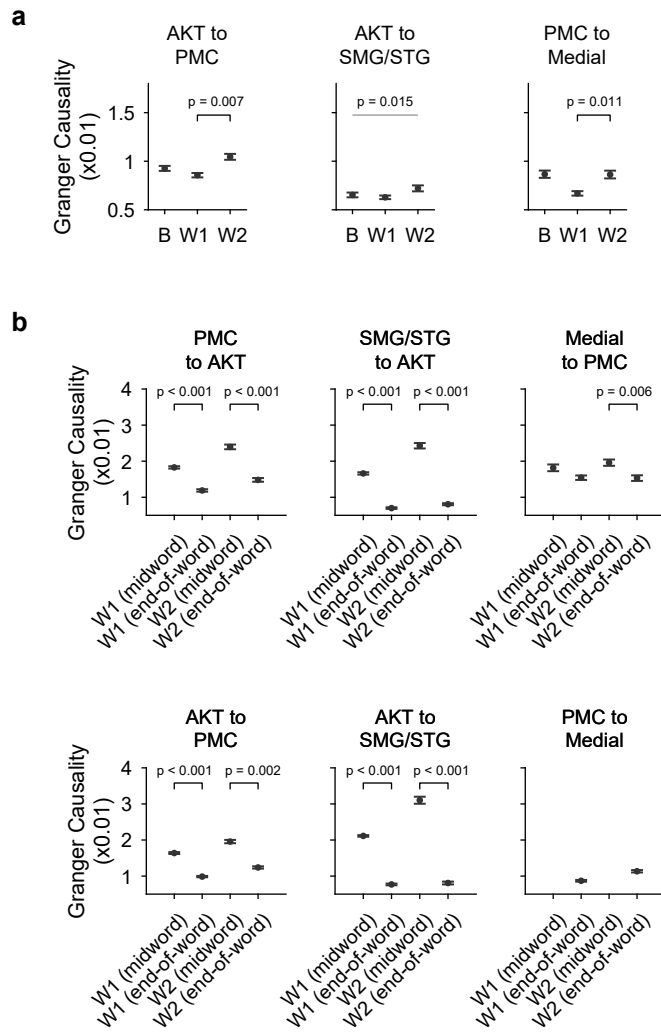


Extended Data Fig. 5 | Spatial location of electrodes showing action related, cue related, and other activity. (a) Similar format as Fig. 3a, c, example electrode showing stop activity not correlated to either stop action or stop cue (referred to as “other”). (b) Location of electrodes belonging to the three types. The black-and-white circles indicate the location of example electrodes shown in Fig. 3a-d and in (a). (c) The proportion of electrodes found in each brain region. PrCG: precentral gyrus; PoCG: postcentral gyrus; IFG: inferior frontal gyrus;

MFG: middle frontal gyrus; Parietal: parietal cortex; STG: superior temporal gyrus. (d) Stop activity from each participant grouped by the types. Gray curve: normalized activity from individual electrodes. Thick colored curve: averaged activity from all electrodes within individual participants (S1-S12) and for all participants (rightmost column). Downward triangles indicate the peak time of the smoothed data shown in the colored curve.

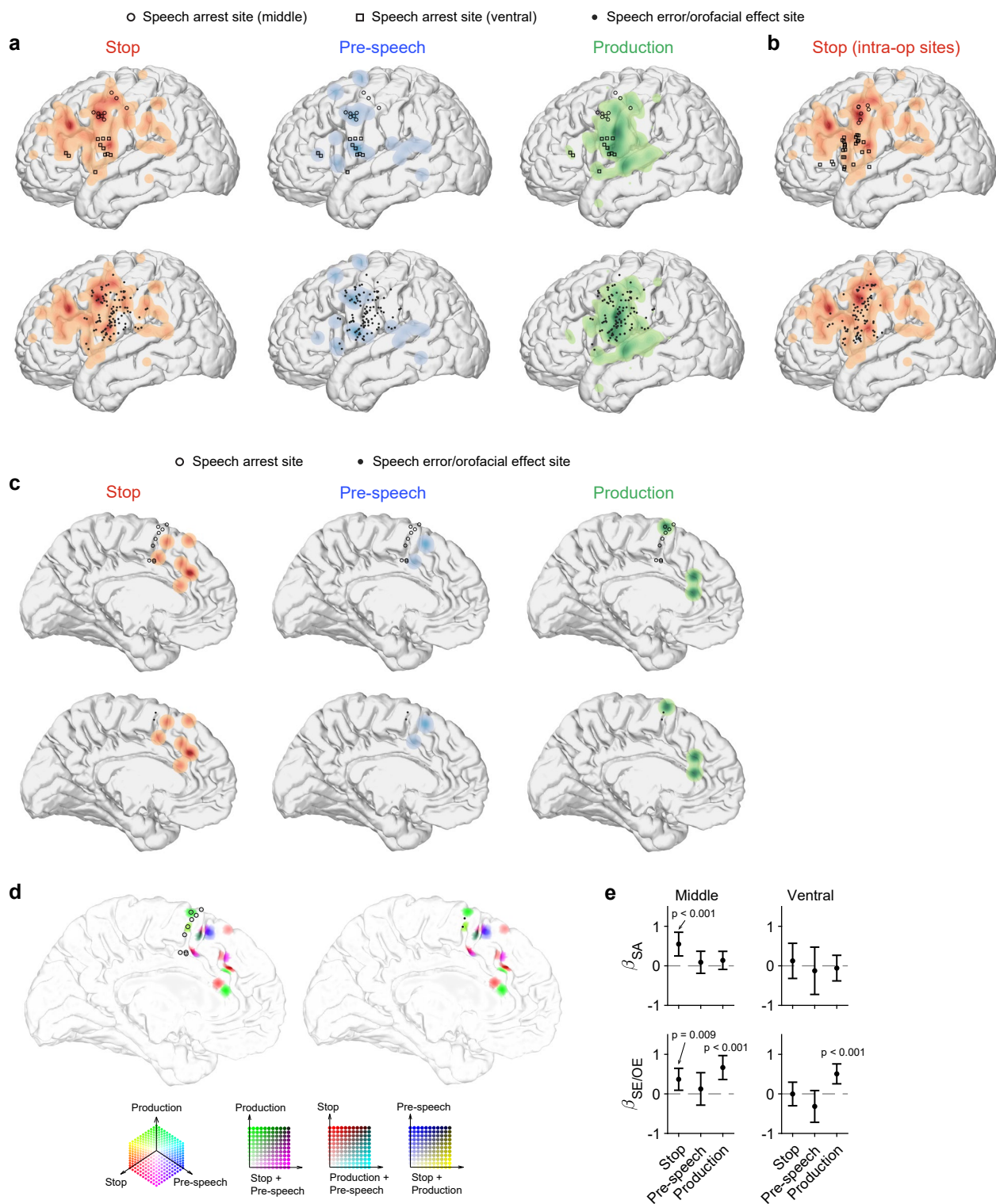


Extended Data Fig. 6 | Spatial location of stop electrodes and electrodes showing strong encoding of AKT features in each participant. Similar format as Fig. 5c. Red: stop electrodes. Green: electrodes with strong encoding of AKT features ($r > 0.2$). Only a few stop electrodes also showed strong encoding of AKT features, indicated by red circles with green borders.



Extended Data Fig. 7 | Granger causality between electrode groups. (a) Similar format as Fig. 5f. Granger causality between groups of stop electrodes and AKT-encoding electrodes (mean \pm s.e.m.), characterized before and after the stop cue. PMC: stop electrodes in the lateral premotor cortex, including the precentral gyrus, IFG, and MFG. AKT: AKT-encoding electrodes without stop activity. SMG/STG: stop electrodes in the supramarginal gyrus and the superior temporal gyrus. Medial: stop electrodes in medial cortical regions. B: baseline window [-0.5, 0]s, W1: window 1 [0, 0.5]s, W2: window 2 [0.5, 1]s. Square brackets indicate significant differences between pairs of windows (adjusted $p = 0.007, 0.011$ for W1-W2 comparisons in the left and right panels, repeated measures ANOVA, post hoc analysis using paired two-sided t-test with the Bonferroni corrections). A horizontal line indicates significant differences across the three windows, but

post hoc analysis did not reveal any pair-wise difference ($p = 0.015$, repeated measures ANOVA). (b) Comparison of Granger causality between midword and end-of-word trials, based on the same data in Fig. 5f and (a). Square brackets indicate significant differences ($p < 0.001$ for W1 and W2 comparisons in the upper left and upper middle panels, $p = 0.006$ for W2 comparison in the upper right panel, $p < 0.001$ for W1 comparison in the bottom left panel, $p = 0.002$ for W2 comparison in the bottom left panel, $p < 0.001$ for W1 and W2 comparisons in the bottom middle panel, two-sample, two-sided t-test). In the bottom right panel, no data point is shown for midword trials as there was no significant Granger causality found between any pairs of electrodes from PMC to medial regions.



Extended Data Fig. 8 | See next page for caption.

Extended Data Fig. 8 | Comparison of the location of stimulation sites and the three types of activity. (a) Left: 2D density map of lateral electrodes with stop activity but no pre-speech or production activity, shown on an average brain, overlaid with speech arrest sites (top) and speech error/orofacial effect sites (bottom). Middle: 2D density map of lateral electrodes with pre-speech activity but no stop or production activity, overlaid with the same stimulation sites as in (a). Right: 2D density map of electrodes with production activity but no stop or pre-speech activity, overlaid with the same stimulation sites as in (a). (b) Similar to the left column in (a), the same density map of stop activity, overlaid with speech arrest sites (top) and speech error/orofacial effect sites (bottom) found in a separate dataset of intra-operative mapping. Note that the postcentral gyrus may not be as often stimulated intra-operatively as the precentral gyrus and inferior frontal gyrus. (c) Similar format as (a), for the medial side electrodes. (d) Similar format as Fig. 7c, speech arrest sites (left) and speech error/orofacial effect sites (right) overlaid on the activation map on the medial side. (e) Related to Fig. 7d, coefficients for the model predictors (mean \pm 95% confidence interval) when the predictors are calculated based on averaged t-value without setting

the t-value of non-significant electrodes to zero (speech arrest model, middle cluster, fixed effect: $\beta_{\text{Stop}} = 0.55, t(209) = 3.61, p < 0.001$, two-sided t-test, 95% confidence interval (CI) = [0.25, 0.85]; $\beta_{\text{Pre-speech}} = 0.09, t(209) = 0.63, p = 0.529$, two-sided t-test, 95% CI = [-0.19, 0.37]; $\beta_{\text{Production}} = 0.14, t(209) = 1.19, p = 0.237$, two-sided t-test, 95% CI = [-0.09, 0.37]). The results are largely the same as Fig. 7d, except that for the middle cluster, both stop and production activity had a significant effect on predicting speech error/orofacial effect (speech error/orofacial effect model, middle cluster, fixed effect: $\beta_{\text{Stop}} = 0.37, t(209) = 2.62, p = 0.009$, two-sided t-test, 95% CI = [0.09, 0.65]; $\beta_{\text{Pre-speech}} = 0.13, t(209) = 0.60, p = 0.548$, two-sided t-test, 95% CI = [-0.29, 0.54]; $\beta_{\text{Production}} = 0.67, t(209) = 4.34, p < 0.001$, two-sided t-test, 95% CI = [0.36, 0.97]; ventral cluster, fixed effect: $\beta_{\text{Stop}} = -0.003, t(127) = -0.02, p = 0.986$, two-sided t-test, 95% CI = [-0.30, 0.30]; $\beta_{\text{Pre-speech}} = -0.32, t(127) = -1.57, p = 0.120$, two-sided t-test, 95% CI = [-0.72, 0.08]; $\beta_{\text{Production}} = 0.51, t(127) = 3.98, p < 0.001$, two-sided t-test, 95% CI = [0.25, 0.76]). However, the coefficient of production activity is higher than that of stop activity, suggesting that production activity had a stronger contribution to speech error/orofacial effect than stop activity.

Corresponding author(s): Edward Chang

Last updated by author(s): Dec 18, 2024

Reporting Summary

Nature Portfolio wishes to improve the reproducibility of the work that we publish. This form provides structure for consistency and transparency in reporting. For further information on Nature Portfolio policies, see our [Editorial Policies](#) and the [Editorial Policy Checklist](#).

Statistics

For all statistical analyses, confirm that the following items are present in the figure legend, table legend, main text, or Methods section.

n/a Confirmed

- The exact sample size (n) for each experimental group/condition, given as a discrete number and unit of measurement
- A statement on whether measurements were taken from distinct samples or whether the same sample was measured repeatedly
- The statistical test(s) used AND whether they are one- or two-sided
Only common tests should be described solely by name; describe more complex techniques in the Methods section.
- A description of all covariates tested
- A description of any assumptions or corrections, such as tests of normality and adjustment for multiple comparisons
- A full description of the statistical parameters including central tendency (e.g. means) or other basic estimates (e.g. regression coefficient) AND variation (e.g. standard deviation) or associated estimates of uncertainty (e.g. confidence intervals)
- For null hypothesis testing, the test statistic (e.g. F , t , r) with confidence intervals, effect sizes, degrees of freedom and P value noted
Give P values as exact values whenever suitable.
- For Bayesian analysis, information on the choice of priors and Markov chain Monte Carlo settings
- For hierarchical and complex designs, identification of the appropriate level for tests and full reporting of outcomes
- Estimates of effect sizes (e.g. Cohen's d , Pearson's r), indicating how they were calculated

Our web collection on [statistics for biologists](#) contains articles on many of the points above.

Software and code

Policy information about [availability of computer code](#)

Data collection MATLAB R2014a, Tucker-Davis Technologies Synapse Software

Data analysis MATLAB R2019a, MATLAB R2023b, Audacity, Python 3.7, mne 0.21, Package from [https://github.com/bootphon/articulatory_inversion], Liblinear package [https://github.com/cjlin1/liblinear], MVGC Toolbox. The code for data analysis is available at https://doi.org/10.5281/zenodo.14513144

For manuscripts utilizing custom algorithms or software that are central to the research but not yet described in published literature, software must be made available to editors and reviewers. We strongly encourage code deposition in a community repository (e.g. GitHub). See the Nature Portfolio [guidelines for submitting code & software](#) for further information.

Data

Policy information about [availability of data](#)

All manuscripts must include a [data availability statement](#). This statement should provide the following information, where applicable:

- Accession codes, unique identifiers, or web links for publicly available datasets
- A description of any restrictions on data availability
- For clinical datasets or third party data, please ensure that the statement adheres to our [policy](#)

The data that support the main findings of this study are available via Zenodo at <https://doi.org/10.5281/zenodo.14512660>. Raw data are available from the corresponding author upon request.

Research involving human participants, their data, or biological material

Policy information about studies with [human participants or human data](#). See also policy information about [sex, gender \(identity/presentation\), and sexual orientation](#) and [race, ethnicity and racism](#).

Reporting on sex and gender	Sex information for participants is reported in the "Methods" section of the manuscript. Sex and gender were not considered in the study design as we do not expect it to affect neural activity for speech production control.
Reporting on race, ethnicity, or other socially relevant groupings	Socially relevant variables are not used in this study. We do not expect them to affect neural activity for speech production control.
Population characteristics	Data from the speech stopping task included 13 participants (4 male, 9 female, mean ± std. age: 30 ± 8 years). All participants were neurosurgical patients at UCSF undergoing intracranial monitoring for intractable epilepsy.
Recruitment	Patients who were scheduled for intracranial epilepsy monitoring were asked whether they were willing to take part in fundamental research studies during the implantation-phase of their hospitalization. The placements of the electrode grids were determined solely by clinical needs. Written informed consent was acquired before surgery. Additional verbal consent was also acquired at the beginning and during the breaks of each research session.
Ethics oversight	The study protocol was approved by the Institutional Review Board at the University of California, San Francisco (UCSF).

Note that full information on the approval of the study protocol must also be provided in the manuscript.

Field-specific reporting

Please select the one below that is the best fit for your research. If you are not sure, read the appropriate sections before making your selection.

Life sciences Behavioural & social sciences Ecological, evolutionary & environmental sciences

For a reference copy of the document with all sections, see nature.com/documents/nr-reporting-summary-flat.pdf

Life sciences study design

All studies must disclose on these points even when the disclosure is negative.

Sample size	No explicit sample size calculation was performed. The amount of data collected from each participant was purely dependent on their clinical treatment schedule and the amount of time each participant was willing to volunteer for the study. The sample size (n = 13 participants) is greater than previous studies from our lab that successfully use intracranial ECoG (e.g. Chang et al. Nature Neuroscience 2010, n = 4; Mesgarani et al. Science 2014, n = 6; Tang et al. Science 2017, n = 10). The number of task-relevant electrodes (n = 281 in total) is also comparable to similar studies using high-density, broad-coverage ECoG grids.
Data exclusions	No data were excluded from analysis.
Replication	No explicit attempt at replication of the results reported has been undertaken. However, the behavioral and neural results were replicated in all participants individually.
Randomization	All experimental manipulations were conducted as a within-participant design. Stop cues in the speech stopping task were presented with randomized time delays. Sentences in the sentence reading task were presented in randomized order.
Blinding	Blinding was not relevant for this study. The experimenter was not aware of the cue timing or target sentence in upcoming trials. The experimenter did not interact with the participant in the middle of the tasks.

Reporting for specific materials, systems and methods

We require information from authors about some types of materials, experimental systems and methods used in many studies. Here, indicate whether each material, system or method listed is relevant to your study. If you are not sure if a list item applies to your research, read the appropriate section before selecting a response.

Materials & experimental systems

n/a	Involved in the study
<input checked="" type="checkbox"/>	Antibodies
<input checked="" type="checkbox"/>	Eukaryotic cell lines
<input checked="" type="checkbox"/>	Palaeontology and archaeology
<input checked="" type="checkbox"/>	Animals and other organisms
<input type="checkbox"/>	Clinical data
<input checked="" type="checkbox"/>	Dual use research of concern
<input checked="" type="checkbox"/>	Plants

Methods

n/a	Involved in the study
<input checked="" type="checkbox"/>	ChIP-seq
<input checked="" type="checkbox"/>	Flow cytometry
<input checked="" type="checkbox"/>	MRI-based neuroimaging

Clinical data

Policy information about [clinical studies](#)

All manuscripts should comply with the ICMJE [guidelines for publication of clinical research](#) and a completed [CONSORT checklist](#) must be included with all submissions.

Clinical trial registration [ClinicalTrials.gov NCT05876910](#)

Study protocol [A description of the study can be found at https://classic.clinicaltrials.gov/ct2/show/NCT05876910](https://classic.clinicaltrials.gov/ct2/show/NCT05876910)

Data collection Data were collected at the UCSF Medical Center

Outcomes Not relevant for this study